

F
N
P

JOURNAL
OF
FOOD
PROCESS
ENGINEERING

D.R. HELDMAN
and
R.P. SINGH
COEDITORS

FOOD & NUTRITION
PRESS, INC.

VOLUME 11, NUMBER 1

1989

JOURNAL OF FOOD PROCESS ENGINEERING

Coeditors: **D.R. HELDMAN**, National Food Processors Association, 1401 New York Ave., N.W., Washington, D.C.
R.P. SINGH, Agricultural Engineering Department, University of California, Davis, California

Editorial

Board:

A.L. BRODY, Princeton, New Jersey
SOLKE, BRUIN, Vlaardingen, 1 Nederland
A. CALVELO, La Plata, Argentina
M. CHERYAN, Urbana, Illinois
J.P. CLARK, Chicago, Illinois
R.L. EARLE, Palmerston, North New Zealand
B. HALLSTROM, Lund, Sweden
J.M. HARPER, Fort Collins, Colorado
H. HAYASHI, Tokyo, Japan
M. KAREL, New Brunswick, New Jersey
H.G. KESSLER, Freising-Weihenstephan, F.R. Germany
C.J. KING, Berkeley, California
J.L. KOKINI, New Brunswick, New Jersey
M. LEMAGUER, Edmonton, Alberta, Canada
R.G. MORGAN, Glenview, Illinois
M. PELEG, Amherst, Massachusetts
M.A. RAO, Geneva, New York
I. SAGUY, Minneapolis, Minnesota
S.K. SASTRY, Columbus, Ohio
W.E.L. SPIESS, Karlsruhe, Germany
J.F. STEFFE, East Lansing, Michigan

All articles for publication and inquiries regarding publication should be sent to DR. D.R. HELDMAN, COEDITOR, *Journal of Food Process Engineering*, National Food Processors Association, 1401 New York Ave., N.W., Washington, D.C. 20005 USA; or DR. R.P. SINGH, COEDITOR, *Journal of Food Process Engineering*, University of California, Davis, Department of Agricultural Engineering, Davis, CA 95616 USA.

All subscriptions and inquiries regarding subscriptions should be sent to Food & Nutrition Press, Inc., 6527 Main Street, P.O. Box 374, Trumbull, CT 06611 USA.

One volume of four issues will be published annually. The price for Volume 11 is \$85.00 which includes postage to U.S., Canada, and Mexico. Subscriptions to other countries are \$102.00 per year via surface mail, and \$111.00 per year via airmail.

Subscriptions for individuals for their own personal use are \$65.00 for Volume 11 which includes postage to U.S., Canada, and Mexico. Personal subscriptions to other countries are \$82.00 per year via surface mail, and \$91.00 per year via airmail. Subscriptions for individuals should be sent direct to the publisher and marked for personal use.

The *Journal of Food Process Engineering* (ISSN: 0145-8876) is published quarterly (March, June, September and December) by Food & Nutrition Press, Inc.—Office of Publication is 6527 Main Street, P.O. Box 374, Trumbull, Connecticut 06611 USA. (Current issue is June 1989.)

Second class postage paid at Bridgeport, CT 06602.

POSTMASTER: Send address changes to Food & Nutrition Press, Inc., 6527 Main Street, P.O. Box 374, Trumbull, CT 06611.

JOURNAL OF FOOD PROCESS ENGINEERING

JOURNAL OF FOOD PROCESS ENGINEERING

- Coeditors:* **D.R. HELDMAN**, National Food Processors Association, 1401 New York Ave., N.W., Washington, D.C.
R.P. SINGH, Agricultural Engineering Department, University of California, Davis, California.
- Editorial Board:* **A.L. BRODY**, Schotland Business Research, Inc., Princeton Corporate Center, 3 Independence Way, Princeton, New Jersey
SOLKE, BRUIN, Unilever Research Laboratorium, Vlaardingen, Oliver van Noortland 120 postbus 114, 3130 AC Claardingen 3133 AT Vlaardingen, 1 Nederland
A. CALVELO, Centro de Investigacion y Desarrollo en Criotechnologia de Alimentos, Universidad Nacional de la Plata, Argentina
M. CHERYAN, Department of Food Science, University of Illinois, Urbana, Illinois.
J.P. CLARK, Epstein Process Engineering, Inc., Chicago, Illinois
R.L. EARLE, Department of Biotechnology, Massey University, Palmerston North, New Zealand
B. HALLSTROM, Food Engineering Chemical Center, S-221 Lund, Sweden
J.M. HARPER, Agricultural and Chemical Engineering Department, Colorado State University, Fort Collins, Colorado
H. HAYASHI, Snow Brand Milk Products Co., Ltd., Shinjuku, Tokyo, Japan
M. KAREL, Department of Food Science, Rutgers, The State University, Cook College, New Brunswick, New Jersey
H.G. KESSLER, Institute for Dairy Science and Food Process Engineering, Technical University Munich, Freising-Weihenstephan, F.R. Germany
C.J. KING, Department of Chemical Engineering, University of California, Berkeley, California
J.L. KOKINI, Department of Food Science, Rutgers University, New Brunswick, New Jersey
M. LEMAGUER, Department of Food Science, University of Alberta, Edmonton, Canada
R.G. MORGAN, Kraft, Inc., Glenview, Illinois
M. PELEG, Department of Food Engineering, University of Massachusetts, Amherst, Massachusetts
M.A. RAO, Department of Food Science and Technology, Institute for Food Science, New York State Agricultural Experiment Station, Geneva, New York
I. SAGUY, The Pillsbury Co., Minneapolis, Minnesota
S.K. SASTRY, Department of Agricultural Engineering, Ohio State University, Columbus, Ohio
W.E.L. SPIESS, Bundesforschungsanstalt fuer Ernaehrung, Karlsruhe, Germany
J.F. STEFFE, Department of Agricultural Engineering, Michigan State University, East Lansing, Michigan

Journal of
FOOD PROCESS ENGINEERING

VOLUME 11
NUMBER 1

Coeditors: D.R. HELDMAN
 R.P. SINGH

FOOD & NUTRITION PRESS, INC.
TRUMBULL, CONNECTICUT 06611 USA

© Copyright 1989 by
Food & Nutrition Press, Inc.
Trumbull, Connecticut USA

All rights reserved. No part of this publication may be reproduced, stored in a retrieval system or transmitted in any form or by any means: electronic, electrostatic, magnetic tape, mechanical, photocopying, recording or otherwise, without permission in writing from the publisher.

ISSN 0145-8876

Printed in the United States of America

CONTENTS

Conduction Heating of High Moisture Rough Rice II. Safe Temporary Storage V.G. REYES, JR. and V.K. JINDAL	1
The Roast: Nonlinear Modeling and Simulation M.A. TOWNSEND and S. GUPTA	17
A Finite Element Method to Model Steam Infusion Heat Transfer to a Free Falling Film K.L. MCCARTHY and R.L. MERSON	43
A Generalized Viscosity Model for Extrusion of Protein Doughs R.G. MORGAN, J.F. STEFFE and R.Y. OFOLI	55

CONDUCTION HEATING OF HIGH MOISTURE ROUGH RICE

II. SAFE TEMPORARY STORAGE

V.G. REYES, JR. and V.K. JINDAL

*Division of Agricultural and Food Engineering
Asian Institute of Technology
P.O. Box 2754
Bangkok, Thailand 10501*

Accepted for Publication June 27, 1988

ABSTRACT

High temperature conduction heating reduced the fungal growth and prevented the spoilage of freshly harvested high moisture rough rice leading to its safe temporary storage. Heat treatments resulting in fungal mortality levels equal to 90% and higher were found to be satisfactory for general use. Finally, a relationship was developed for estimating the safe storage periods of heat-treated high moisture rough rice based on its moisture content and fungal mortality level achieved with various heat treatments.

INTRODUCTION

High moisture rough rice harvested during the rainy season may be temporarily held back for several days before drying because of the inadequate drying facilities in Southeast Asia. As a result, rough rice at high moisture levels may suffer substantial losses both in quality and quantity due to the rapid growth of microorganisms specifically fungi on or within the grain (Schroeder and Sorenson 1961; Fazli and Schroeder 1966a,b; Schroeder 1967; Mendoza *et al.* 1981; Quitco 1982). A reduction in quality and quantity of rough rice leads to a direct economic loss. Presently available means of extending the safe storage period of high moisture rough rice such as the use of chemical preservatives, controlled atmosphere storage and aeration have been used with limited success (Calderwood and Schroeder 1975; de Padua 1965; Schroeder and Sorenson 1961). Therefore practical as well as economical means of holding high moisture rice awaiting drying need to be developed in view of the increasing importance of the wet season crop.

In the first part of this study, it was reported that conduction heating could effectively arrest the fungal growth in freshly harvested high moisture rough rice while subjecting it to partial drying (Reyes and Jindal 1988). It was also

hypothesized that reduced fungal growth could extend the safe temporary storage of high moisture rice prior to final drying without any quality deterioration. Therefore, the objective of this study was to evaluate the effectiveness of conduction heat treatment in preventing the spoilage of high moisture rough rice while undergoing temporary storage. More specifically, an attempt was made to quantify the effects of heat treatments on the safe holding periods of rough rice based on acceptable criteria of quality deterioration in milled rice.

MATERIALS AND METHODS

Heating Experiments

Freshly harvested high moisture rough rice samples of variety RD-23 were heated in an experimental rotary conduction heating unit. The details of the equipment and experimental procedure are given by Reyes and Jindal (1988). The experimental conditions included the following:

Heating surface temperature	:100, 150 and 200 °C
Moisture content of samples	:In the range of 22.0 to 26.5% w.b.
Exposure duration	:Corresponding to fungal mortality levels of 0, 75, 90 and 95%
Cooling rate	:0.7 °C/min
Storage period	:0, 3, 5, 10 and 15 days

Storage Experiments

After the heat treatment, rough rice samples were allowed to cool to room temperature in plastic containers covered with a perforated aluminum foil to permit the escape of water vapor during cooling. Subsequently the samples were transferred into 2 liter capacity glass bottles with provision for carbon dioxide to escape through the cotton plugs into the atmosphere during storage. The samples were aerated using a simple hand pump every 24 h to prevent the excessive build-up of carbon dioxide in the storage chamber. The samples were stored at room temperature (28–30 °C) during the test period and analyzed for fungal count, head rice yields, and the percentage of discolored kernels in milled rice at intervals of 0, 3, 5, 10 and 15 days.

Measurement of Fungal Activity

The number and proportion of fungi present in rough rice samples were determined by dilution plating assay as described by Flannigan (1977). An indirect

measurement of fungal activity in terms of carbon dioxide production was also carried out using a system first proposed by Steele *et al.* (1969) and described in detail by Reyes (1986). The overall effects of heat treatments were expressed in terms of fungal load ratio (FLR) and fungal mortality level (FML) as defined by Reyes and Jindal (1988).

Milling Quality Evaluation

All rough rice samples (heat-treated and control) were air-dried to 14% moisture content prior to milling. The milling quality was evaluated in terms of the percentage of head rice representing 3/4 of whole kernels size or larger and total milled rice using a standard laboratory procedure (USDA 1977).

Determination of Discolored Kernels

The discolored kernels present in milled rice samples weighing about 20 to 30 g were separated manually and expressed later as a percentage of the total sample weight.

Discoloration of Milled Rice Due to Fungal Infection

A separate subexperiment was conducted to determine the discoloration of milled rice kernels inflicted by specific fungi. Rough rice samples, each weighing approximately 300 g and having moisture content in the range of 24 to 26%, were first sterilized using 2% sodium hypochlorite solution for about a minute and inoculated subsequently with *Helminthosporium*, *Penicillium*, *Aspergillus flavus*, and *Aspergillus niger* species of fungi in glass flasks. Another 300 g of rough rice was placed in a similar flask without inoculation to serve as the control. The samples were incubated for 15 days at room temperature.

RESULTS AND DISCUSSION

Effects of Heat Treatments on Selected Quality Indices of Rough Rice

Table 1 presents the test conditions of heat treatments and the resulting changes in selected quality indices such as final moisture content, fungal load ratio and head rice yields of rough rice samples at the start of the storage experiments. The presented results are average of three replications. As expected, heating surface temperature and the exposure time played a significant role in reducing the fungal load ratio. On the contrary, the head rice yields of heat-treated samples were increased in general perhaps due to the partial gelatinization of starch in rice grains. The head yield ratio increased in the range of 9 to 11% for rough rice having initial moisture content of about 26% w.b. due to

TABLE I.
EXPERIMENTAL CONDITIONS AND QUALITY OF ROUGH RICE SAMPLES
AFTER HEAT TREATMENT

Test number	Initial moisture content (% w.b.)	Heating surface temp. (°C)	Exposure time (min)	Fungal load ratio	Final moisture content (% w.b.)	Head yield (%)	Discolored kernels (%)
1	23.5	200	0.0	1.000	23.5	56.7	0.76
2	23.5	200	0.6	0.855	23.3	57.5	0.76
3	23.5	200	2.2	0.016	22.7	59.8	0.76
4	23.5	200	7.4	0.016	18.2	60.6	0.76
5	22.0	150	0.0	1.000	22.0	47.5	0.75
6	22.0	150	1.6	0.460	21.7	48.0	0.75
7	22.0	150	5.3	0.018	20.4	48.8	0.75
8	22.0	150	14.6	0.010	17.6	48.1	0.75
9	22.2	100	0.0	1.000	22.2	47.8	0.68
10	22.2	100	8.2	0.326	21.7	48.5	0.68
11	22.2	100	19.8	0.038	20.6	49.7	0.68
12	22.2	100	33.2	0.008	19.3	49.3	0.68
13	26.4	200	0.0	1.000	26.4	50.7	0.20
14	26.4	200	0.8	0.553	25.2	54.8	0.20
15	26.4	200	3.0	0.162	24.1	59.3	0.20
16	26.4	200	9.1	0.084	19.5	60.0	0.20
17	27.3	150	0.0	1.000	27.3	50.1	0.42
18	27.3	150	2.1	0.475	26.4	55.1	0.42
19	27.3	150	6.5	0.190	25.2	60.8	0.42
20	27.3	150	16.6	0.031	21.5	60.6	0.42
21	26.3	100	0.0	1.000	26.3	51.6	0.48
22	26.3	100	9.8	0.281	25.1	55.5	0.48
23	26.3	100	22.0	0.187	24.8	58.6	0.48
24	26.3	100	40.0	0.074	22.7	60.3	0.48

conduction heating. The corresponding increase in head yield ratio of rice with initial moisture content of about 22% w.b. was found to be ranging from 2 to 4%. The beneficial effects of heat treatments were thus obvious in terms of reduced fungal activity and improved milling quality. It appeared that heat treatments corresponding to a fungal mortality level in the range of 0.90 to .095 (0.10 to 0.05 FLR) resulted in a final moisture content of rough rice about 3 to 6% w.b. lower than the initial value depending upon the heating surface temperature.

Changes in Head Rice Yields During Temporary Storage

In general the head rice yield of heat-treated and control samples decreased progressively with an increase in the storage period in all experiments. However, rough rice samples which were heat-treated to at least 90% fungal mortality level showed a marked reduction in the proportions of brokens and thus higher head yields during milling in comparison with that of control sample at the start of the storage experiments. In addition, the effect of prolonged storage was found to be less severe for heat-treated samples in comparison with the control samples. The reduction in head yield appeared to be linearly related with the storage period in all twenty-four experiments by the following equation:

$$\text{HYS} = \text{HYC} [1 - b (\text{SD})] \quad (1)$$

where HYS = head rice yield of rough rice during storage, %

HYC = head rice yield of control sample at the start of storage experiments, %

SD = storage period, day

b = regression coefficient

Equation 1 represented the percent change in head rice yields of rough rice relative to the control sample. The values of regression coefficient b in Eq. 1 represented the reduction in head yield ratio per day during the storage and are presented in Table 2.

Unheated rough rice samples having initial moisture contents in the ranges of 22–23% and 26–27% showed a reduction in head rice yield of about 0.45% and 1.31%, respectively for each day of storage. However, similar rough rice samples when subjected to heat treatments corresponding to at least 95% fungal mortality level showed about 0.14% and 0.32% reduction in head rice yield per day for low and high moisture content samples, respectively. The higher rate of reduction in head rice yield of control or unheated samples could be attributed to an increase in the damaged kernels due to higher fungal activity during the temporary storage. Heat-treated rough rice samples produced higher head yields indicating low levels of damage incurred under similar storage conditions.

TABLE 2.
PARAMETERS OF THE EQUATIONS RELATING HEAD RICE YIELD
AND PERCENT DISCOLORED KERNELS WITH STORAGE TIME

Test number	Eq. 1		Eq. 2		
	b	R*	a ₁	b ₁	R*
1	0.00272	0.950	0.0035550	1.4225	0.900
2	0.00243	0.900	0.0000041	4.0200	0.980
3	0.00162	0.910	0.0001507	1.8800	0.953
4	0.00080	0.950	0.0005258	0.8989	0.978
5	0.00648	0.930	0.0009878	1.8600	0.971
6	0.00592	0.900	0.0022790	1.1000	0.880
7	0.00219	0.890	0.0000390	2.0656	0.982
8	0.00106	0.900	0.0000863	1.2159	0.998
9	0.00425	0.910	0.0004351	2.1600	0.996
10	0.00408	0.860	0.0001610	1.9600	0.998
11	0.00241	0.940	0.0007016	0.9117	0.850
12	0.00220	0.920	0.0001458	1.3161	0.900
13	0.01595	0.930	0.0482190	0.5315	0.920
14	0.01114	0.950	0.0009663	2.0015	0.996
15	0.01082	0.890	0.0000023	3.9000	0.998
16	0.00199	0.950	0.0000008	4.0600	0.994
17	0.01389	0.920	0.0581920	0.3840	0.943
18	0.01343	0.960	0.0042281	1.2850	0.923
19	0.01697	0.950	0.0002913	2.0600	0.968
20	0.00085	0.930	0.0000338	2.3120	0.900
21	0.00937	0.900	0.0095140	1.1960	0.900
22	0.00746	0.910	0.0016850	1.6200	0.939
23	0.01262	0.930	0.0004949	2.0100	0.979
24	0.00678	0.900	0.0000124	3.2000	0.965

*Correlation coefficient

Discoloration of Milled Rice During Temporary Storage

The effect of heat treatments in suppressing the fungal growth was more pronounced in terms of discolored milled rice kernels appearing during the storage period. It was observed that the discoloration in high moisture rice increased exponentially with the length of storage period and could be represented by the following equation:

$$DS = DC + (1 - \exp[-a_1 (SD)^{b_1}]) \quad (2)$$

where DS = weight fraction of discolored kernels in rough rice during storage, decimal

DC = weight fraction of discolored kernels in control sample initially, decimal

a₁, b₁ = regression coefficients

Typical plots of this relationship are shown in Fig. 1 and 2. The values of regression coefficients a₁ and b₁ are also presented in Table 2.

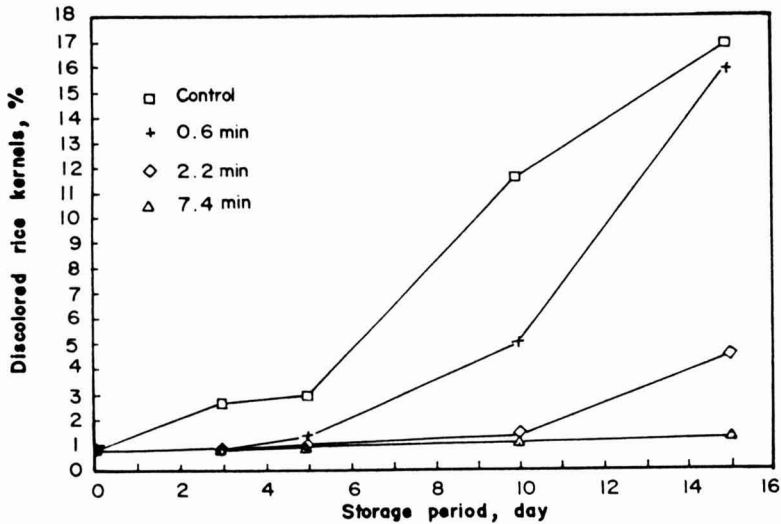


FIG. 1. DISCOLORATION OF MILLED RICE KERNELS AS A FUNCTION OF STORAGE PERIOD OF ROUGH RICE HAVING 22% INITIAL MOISTURE CONTENT WHEN HEATED FOR DIFFERENT EXPOSURE TIMES USING 200°C SURFACE TEMPERATURE

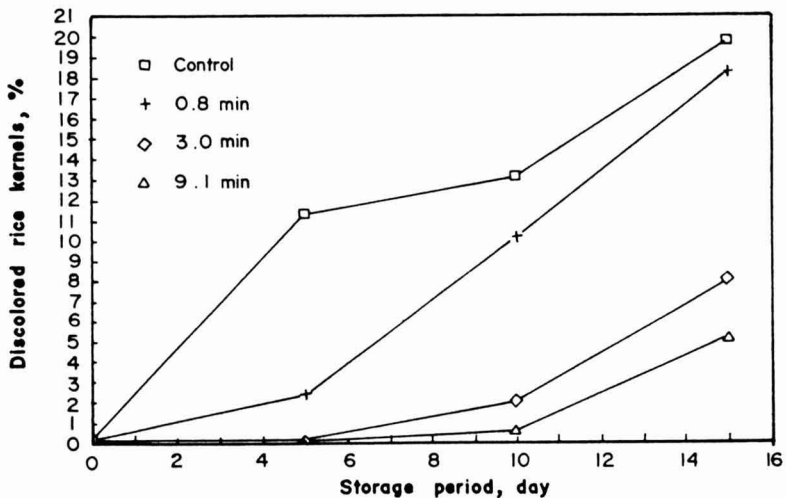


FIG. 2. DISCOLORATION OF MILLED RICE KERNELS AS A FUNCTION OF STORAGE PERIOD OF ROUGH RICE HAVING 26% INITIAL MOISTURE CONTENT WHEN HEATED FOR DIFFERENT EXPOSURE TIMES USING 200°C SURFACE TEMPERATURE

During the storage of both heat-treated and control samples, it was observed that the proportion of discolored milled rice kernels was increased at a much faster rate in comparison with the reduction in head rice yields. This implied that the appearance of discolored kernels will be the limiting factor affecting the safe storage period of high moisture rice and hence its market grade subsequently.

Safe Holding Periods for High Moisture Rough Rice

In order to estimate the safe holding period of high moisture rice, the acceptable limits of reduction in head rice yield and an increase in the proportion of discolored kernels were selected based on one-step reduction in U.S. market grade quality (USDA 1977). Accordingly the time required for a 3% reduction in the head rice yield or a 1.5% increase in discolored kernels was defined as the safe storage period. The safe storage periods were estimated from Eq. 1 and 2, respectively based on the reduction in head yield and an increase in discolored kernels, respectively as shown in Table 3. The table shows that the limiting factor affecting the market grade of milled rice would be the percentage of discolored kernels because of its greater sensitivity to loss in quality during temporary storage of high moisture rice.

Unheated rice samples with initial moisture content of approximately 22 to 23.5% were lowered one step in the market grade within 3 to 5 days. Whereas rough rice with moisture content of about 26% showed a safe holding period of about one day only. These observations are in line with the findings of McNeal (1960) who reported storage damage in rough rice having 24% moisture content and above at the end of the first day and for rice having 21 to 23.9% moisture content between third and fourth day.

In general heat treatments corresponding to 90% fungal mortality in rice samples having moisture in the range of 22 to 23.5% resulted in an increase of about 10 to 23 days in the safe holding periods. For example, heating of rice for 2.2 min using surface temperature of 200°C resulted in safe storage period of about 12 days. On the other hand, rice having an initial moisture content of 26% when heated to achieve approximately 90 to 95% fungal mortality level (for about 3 to 9 min using 200°C surface temperature) showed an increase of about 10 to 12 days in safe storage period. This temporary storage of rice should enable effective utilization of dryer capacity through proper scheduling of heat treatment and drying operations.

Using multiple regression analysis, a relationship was developed for estimating the safe storage period based on the fungal load ratio and final moisture content of rough rice attained as a result of various heat treatments as follows:

$$\begin{aligned} \ln \text{SSD} = & 7.1223 - 0.7731 \exp(\text{FLR}) \\ & - 5.466 \times 10^{-12} \exp(\text{FMC}) - 0.1616(\text{FMC}) \end{aligned} \quad (3)$$

where SSD = safe storage period, day

FLR = fungal load ratio, (FC_i/FC_o), decimal

FC_i = fungal count in heat-treated rough rice sample, colonies/g

FC_o = fungal count in unheated rough rice sample (control), colonies/g

FMC = final moisture content of rough rice after heat treatment, % w.b.

TABLE 3.
SAFE STORAGE PERIODS FOR HIGH MOISTURE ROUGH RICE

Test number	Safe storage period (days) based on	
	Head rice yield	Discolored kernels
1	19.5	2.7
2	27.3	7.7
3	63.5	11.6
4	142.5	26.0
5	9.7	4.3
6	12.2	5.6
7	40.2	17.9
8	71.3	70.0
9	14.7	5.2
10	18.7	10.2
11	40.0	29.0
12	41.6	34.0
13	3.7	0.1
14	11.7	4.0
15	18.1	9.5
16	103.5	11.4
17	4.3	0.0
18	10.9	2.7
19	13.3	6.8
20	262.4	14.0
21	6.2	1.5
22	16.7	3.9
23	13.6	5.5
24	28.7	9.2

The coefficient of determination and standard error of estimate for Eq. 3 were found to be 0.90 and 0.58, respectively and considered satisfactory based on the experimental limitations. Equation 3 clearly showed that safe holding period of rough rice was strongly influenced by the grain moisture content and fungal load ratio at the start of storage. Further analysis showed that the coefficient of determination was about 0.50 without moisture content as a parameter, thus indicating a high correlation of safe storability of rough rice with the fungal activity.

Carbon Dioxide Production by Heat-Treated Rough Rice Samples

An attempt was made to study the possible relationship between the carbon dioxide production by heat treated rough rice samples during storage with their safe holding periods. The production of carbon dioxide by rice samples could be attributed to the fungal respiration since the viability of the grains was reduced almost to zero level due to high temperature conduction heating. The carbon dioxide production was expressed in terms of an equivalent dry matter loss (EDML) using a conversion factor of 1.46 g CO₂ per g of EDML as recommended by Seib *et al.* (1980) and related with the storage period by the following equation:

$$\text{EDML} = a_2 + b_2 (\text{SD}) + c_2 (\text{SD})^2 \quad (4)$$

where EDML = equivalent dry matter loss, %

SD = storage period, day

a,b,c = regression coefficients

The typical effects of heat treatment on EDML are illustrated in Fig. 3 and 4. The values of regression coefficients a, b and c are given in Table 4. Very low and stable rates of respiration were observed with high moisture rough rice samples heat-treated for about 2 to 3 min using heating surface temperature of 200 °C. These results showed that rough rice having initial moisture content in the range of 18 to 22.5% fell in market grade during storage when EDML was about 0.12% or higher. The corresponding value of EDML in higher moisture content range of 22.5 to 27% was found to be 0.20%. These results are supported by Seib *et al.* (1980) who reported that a dry matter loss of more than 0.25% reduced the market grade of rough rice at 22% moisture content. The limits for EDML obtained in this study during the maximum safe storage period appear to be somewhat stringent. This was perhaps due to a drastic reduction in respiration rate of rough rice samples after the heat treatment and the shorter safe storage periods based on a relatively more sensitive criterion of the discoloration of milled rice used in the present study.

The Role of Fungi in Discoloration of Milled Rice

The results from a separate subexperiment showed that the fungi *Helminthosporium*, *Penicillium*, *Aspergillus flavus*, and *Aspergillus niger* produced pronounced discoloration of the milled rice. The discoloration was probably due to the action of fungus metabolites on the pigments within the rice bran and/or by pigments synthesized by molds themselves (Schroeder and Sorenson 1961). It was revealed that the growth of specific microorganisms in the mass of grain if left unchecked could cause discoloration in the following forms:

a. yellowish brown to black - by *Helminthosporium*, *Penicillium*, and *Aspergillus niger*.

b. light yellow to yellowish green color — by *Aspergillus flavus*.

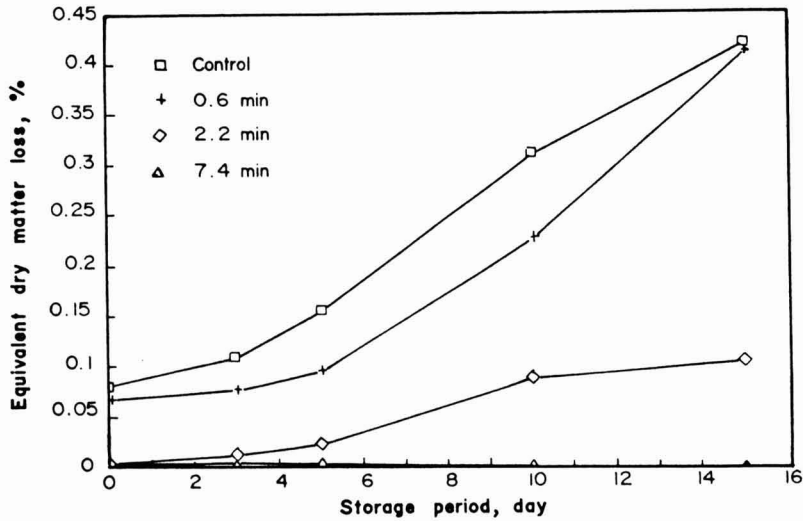


FIG. 3. EQUIVALENT DRY MATTER LOSS AS A FUNCTION OF STORAGE PERIOD OF ROUGH RICE HAVING 22% INITIAL MOISTURE CONTENT WHEN HEATED FOR DIFFERENT EXPOSURE TIMES USING 200°C SURFACE TEMPERATURE

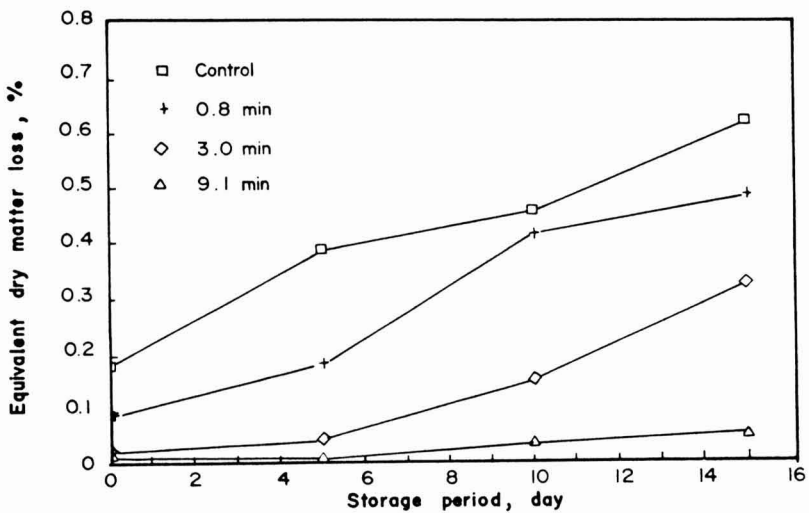


FIG. 4. EQUIVALENT DRY MATTER LOSS AS A FUNCTION OF STORAGE PERIOD OF ROUGH RICE HAVING 26% INITIAL MOISTURE CONTENT WHEN HEATED FOR DIFFERENT EXPOSURE TIMES USING 200°C SURFACE TEMPERATURE

TABLE 4.
PARAMETERS OF EQUATION 4 RELATING EQUIVALENT DRY MATTER LOSS
IN ROUGH RICE SAMPLES AND STORAGE TIME

Test number	a ₂	b ₂	c ₂	R*
1	0.0639	0.0186	0.0004	0.993
2	0.0607	0.0003	0.0016	0.999
3	0.0000	0.0057	0.0001	0.969
4	0.0006	0.0000	0.0000	0.996
5	0.0748	0.0102	0.0003	0.998
6	0.0183	0.0072	0.0013	0.991
7	0.0000	0.0029	0.0002	0.944
8	0.0020	-0.0011	0.0002	0.992
9	0.0754	0.0295	-0.0009	0.977
10	0.0000	0.0205	-0.0003	0.913
11	0.0003	0.0009	0.0002	0.990
12	0.0000	0.0015	0.0001	0.996
13	0.1859	0.0348	-0.0005	0.924
14	0.0722	0.0314	-0.0002	0.988
15	0.0193	-0.0018	0.0015	0.979
16	0.0077	0.0004	0.0002	0.999
17	0.2131	0.0366	-0.0007	0.982
18	0.0334	0.0745	-0.0020	0.981
19	0.0000	0.0356	0.0005	0.971
20	0.0000	0.0078	0.0001	0.935
21	0.1893	0.0423	-0.0009	0.964
22	0.0237	0.0854	-0.0028	0.955
23	0.0000	0.0631	-0.0003	0.981
24	0.0000	0.0030	0.0016	0.971

*Correlation coefficient

TABLE 5.
MILLED RICE APPEARANCE AND HEAD YIELDS OBTAINED FROM
ROUGH RICE SAMPLES INOCULATED WITH SPECIFIC FUNGI

Fungi	Appearance	Head rice yield (%)
Control	none	56.40
<u>Helminthosporium</u>	brown to black	30.13
<u>Penicillium</u>	brown to black	29.98
<u>As. flavus</u>	light yellow to yellow green	42.18
<u>As. niger</u>	brown to black	39.86

In addition, the invasion of these specific fungi in rice grains resulted in reduced head rice yields (Table 5). The rough rice samples inoculated with *Helminthosporium*, *Penicillium*, and *Aspergillus niger* showed a drastic reduction in head rice yields.

Helminthosporium (a field fungi), together with *Penicillium* were the most common fungi in newly harvested rough rice. During heat treatment, these fungi were either eliminated or reduced to a very low level (Reyes and Jindal 1988). Therefore heat treatment of high moisture rice samples effectively reduced the fungal growth and occurrence of damaged kernels during the temporary storage.

SUMMARY AND CONCLUSIONS

This study showed that high-temperature short-time conduction heating of freshly harvested high moisture rice could effectively extend its safe holding period prior to final drying without appreciable damage to grain quality.

Safe holding periods of heat-treated rice samples were determined based upon an acceptable level of reduction in head rice yield and an increase in the proportion of discolored kernels. A relationship was developed for estimating the safe storage period of high moisture rice in terms of reduction in fungal activity and the moisture content after the heat treatment.

The following specific conclusions were drawn based on the results of this study:

(1) Heat treatments reduced the fungal growth and hence the spoilage in freshly harvested high moisture rice leading to its safe temporary storage. The fungal mortality levels close to 90% or slightly higher were found to be satisfactory for general use.

(2) The limiting factor affecting the safe holding period of high moisture rice and thus its market grade was the percentage of discolored kernels.

(3) Heat treatment of rough rice having initial moisture contents in the range of 22 to 26% w.b. using exposure times corresponding to 90% and higher fungal mortality levels resulted in increased safe holding periods of about 10 to 23 days.

(4) The safe storage period of high moisture rice depended upon the fungal load ratio and final moisture content after the heat treatment.

ACKNOWLEDGMENTS

The financial support of United States Agency for International Development, Grant No. 936-5542 for the research project "Heat Sterilization and Accelerated Drying of High Moisture Rice for Safe Storage" is gratefully acknowledged.

REFERENCES

- CALDERWOOD, D.L. and SCHROEDER, H.W. 1975. Chemical preservatives for maintaining moist rice in storage. Texas Agricultural Experiment Station Progress Report, 6 p.
- DE PADUA, D.B. 1965. High moisture storage of rough rice by control environmental gas. Ph.D. Thesis, Michigan State University, East Lansing, MI.
- FAZLI, S.F.I. and SCHROEDER, H.W. 1966a. Kernel disinfection of Bluebonnet 50 rice by *Helminthosporium oryzae*. *Phytopathology*. 56, 507-509.
- FAZLI, S.F.I. and SCHROEDER, H.W. 1966b. Effect of kernel disinfection of rice by *Helminthosporium oryzae* on yields and quality. *Phytopathology*. 56, 1003-1005.
- FLANNIGAN, B. 1977. Enumeration of fungi and assay for ability to degrade structural and storage components of grain. In *Biodeterioration Investigation Techniques*, (H. Walters, ed.) pp. 185-199, Applied Science Publishers, Barking, Essex, England.
- MCNEAL, X. 1960. Rice storage: Effect of moisture content, temperature and time on grade, germination and head rice yield. Arkansas Agr. Expt. Station Bull. 621.
- MENDOZA, E.E., RIGOR, A.C. and ABITAL, F.L. 1981. Grain Quality deterioration in on-farm level operation. Paper presented at the Regional Grains Post-Harvest Workshop, Jan. 20-22, Manila, Philippines.
- QUITCO, R.T. 1982. Studies on fungal infections and heating of paddy. In *Paddy deterioration in Humid Tropics*, pp. 52-56, German Agency for Technical Cooperation (GTZ), Eschborn, West Germany.
- REYES, JR., V.G. 1986. Heat treatment of high moisture paddy for temporary storage. D. Eng. Thesis, Asian Institute of Technology, Bangkok, Thailand.
- REYES, JR., V.G. and JINDAL, V.K. 1988. Conduction heating of high moisture rough rice. I. Thermal inactivation of fungi. *J. Food Proc. Eng.* 10, 231.
- SCHROEDER, H.W. 1957. Orange stain, a storage disease of rice caused by *P. puberlum*. *Phytopathology*. 53, 843.
- SCHROEDER, H.W. 1967. Milling quality of Belle Patna Rice in experimental storage: A study on the effect of field fungi on subsequent invasion by storage fungi. *J. Stored Prod. Res.* 3, 29-33.
- SCHROEDER, H.W. and SORENSON, J.W. 1961. Mold development in rough rice as affected by aeration during storage. *Rice J.* 64(7), 6-12 & 21-23.

- SEIB, P.A., PFOST, H.B., SUKABDI, A., RAO, V.G. and BURROUGHS, R. 1980. Spoilage of rough rice measured by the evolution of CO₂. In Proc. 3rd Annual Workshop on Grains Post-Harvest Technology, pp.75-94. Jan. 29-31, Malaysia.
- STEELE, J.L., SAUL, R.A. and HUKILL, W.V. 1969. Deterioration of shelled corn as measured by carbon dioxide production. Trans. Amer. Soc. Agri. Eng. 12, 685-689.
- USDA. 1977. U.S. standards for rough rice, brown rice for processing, and milled rice. USDA Federal Inspection Service, Inspection Div., Washington, DC.

THE ROAST: NONLINEAR MODELING AND SIMULATION

M.A. TOWNSEND¹ and S. GUPTA

*Department of Mechanical and Aerospace Engineering
University of Virginia
Charlottesville, VA 22901*

and

W.H. PITTS

*Consultant
Nashville, TN*

Accepted for Publication September 23, 1988

ABSTRACT

Roasting meat is modeled as a nonlinear variable-property heat transfer. The results are compared with conventional recommendations, and quite a variance is found for roasts which are either long or flat. The effects of initial temperature, aftercooking, and other parameters are evaluated. A companion paper considers optimizing the roasting process for a specified desired doneness profile.

INTRODUCTION

Cooking a roast is basically a nonlinear variable-property heat treatment problem: heating and cooling a roast under a variety of ambient temperature conditions to achieve a desired doneness (profile). The roast problems involves all mechanisms of heat transfer, may have multiple stages, and has substantial latent heats at the phase changes. There can be mass transfer due to vapor pressure differences and mass loss due to boiling; the former is a small effect and the latter occurs mainly at the outer surface in practical roasting. In this paper the roast is modeled and tested. In a companion paper (Townsend *et al.*) this approach is extended to determine optimal time-temperature cooking schedules to achieve a desired doneness profile.

Most cookbooks specify the cooking time for a roast in minutes per pound for a specified doneness, almost invariably at an oven temperature of 325 °F or 350 °F (163 °C or 177 °C). Some cookbooks (Meat Cook Book 1959; Crocker 1969; Rombauer and Becker 1973) group roasts by two or three types or sizes, with slightly different cooking time per pound recommendations for each group.

¹Wilson Professor and Chairman, Department of Mechanical and Aerospace Engineering, University of Virginia, Thornton Hall, McCormick Road, Charlottesville, Virginia 22901, Tel: (804)924-7422.

There may be suggested "adders", e.g., additional cooking time per pound if frozen. Overall, the recommendations may be so broad as to barely provide extreme limits. Even so, there is general agreement that the doneness at a point in a piece of meat is indicated by the highest temperature achieved at that point. Table 1 shows the doneness temperatures for beef; for the other cuts of meat, more often there is a minimum recommended temperature throughout.

TABLE 1.
DONENESS TEMPERATURES
Sources: (Crocker 1969; Rombauer and Becker 1973)

	Temperature
Beef: rare	140°F
medium	160°F
well done	170°F
Veal	170°F
Pork roast (fresh)	185°F
Cured Pork	160°F to 170°F *
Ham, fully cooked	130°F
Lamb	180°F (although Europeans prefer lamb rare, 160°F)

*Slight differences according to source.

In a simplified form, this problem is a natural for practical application of heat transfer principles, and it appears as such in several texts, e.g., (Rohsenow and Choi 1961 p. 130; Kreith 1973 p. 212). The usual assumptions are a homogeneous, isotropic, simple geometric shape with uniform initial temperature throughout, constant properties, and constant heat transfer coefficient in a uniform constant-temperature oven. Disregarded as such things as radiant energy input, surface heat transfer dependence on temperature, variable properties, humidity and orientation, and moisture removal. The solution to the simplified problem with an infinite boundary (not addressing a roast) appeared prior to 1936, as surveyed and presented in (Newman 1936). As will be shown, the simplifying assumptions and shape affect the cooking time considerably.

Subsequently, Klamkin (1962) showed (with some wit) that based on consideration of heat conduction (only) in a "homogeneous, isotropic, homothetic family" of roasts all at the same constant initial temperature placed into identical

constant oven temperatures, the “proper” cooking time θ_c to a given central doneness temperature should follow the proportionality

$$\theta_c \sim (\text{mass})^{2/3} \quad (\text{i})$$

Klamkin did not assume constant thermal properties, and he stated that homogeneity and isotropy are not necessary as long as the only difference between roasts of the family is size.

On the other hand, if surface convection and radiation determine the rate of heat transferred to the roast under the same conditions as Klamkin’s above and dominate conduction in the roast, then the heat transfer rate is proportional to surface area, viz.

$$q_{in} \sim A_s * (\text{mass})^{2/3} \quad (\text{ii})$$

The total heat absorbed Z in $q_{in}\theta_c$.

At the homothetic center of the roast, the temperature (rise) is proportional to

$$\Delta T \sim \frac{Q}{\text{mass}} * c_p \quad (\text{iii})$$

Hence, for a given center temperature, this “proper” cooking time would follow the proportionality

$$\theta_c \sim (\text{mass})^{1/3} \quad (\text{iv})$$

Considering the different mechanisms involved and with a substantial reduction in the number of assumptions, one might intuitively expect a result somewhere between (i) and (iv). Indeed, for the same initial and final conditions and oven as above, for a “homothetic” family and virtually no other assumptions, plotting our results we find a proportionality of

$$\theta_c \sim (\text{mass})^{.50 \text{ to } .55} \quad (\text{v})$$

The exponent varies slightly with length/diameter ratio (see Results) and the nominal values of surface heat transfer coefficient and absorptivity.

This rule is probably not derivable per se, but depends on modeling and simulation (as here) or extensive experimentation. The former is certainly more economical: a good mathematical model provides a cheap and forgiving experiment and reduces the quantity of costly, time-consuming, wasteful, and possibly inconclusive full-scale experimentation.

In this study, the model includes variables which heretofore had been disregarded or treated as constants. A number of numerical experiments are performed for comparison with other relevant literature e.g., (Newman 1936) as well as with common practice cookbooks. The results are meant to be illustrative, to show the effects of various degrees of thawing, after-cooking, etc. We then address the possibility of alternative cooking programmes - e.g., cooking a frozen roast, the effect of the roast parameters and roasting variables which are critical and should be investigated experimentally, etc.

MODEL

The roast is modeled as a right circular cylinder of length L and diameter D in a uniform temperature field (convection oven). This is a reasonable shape, taking in a range from sausages through most standing roasts (beef, pork, ham) to round steaks and hamburgers. It is mathematically convenient: it can be characterized in terms of length-over-diameter ratio LOD and weight W (or mass m). Throughout, the word "roast" is used to describe this model. In general we shall be primarily considering beef, although by changes in the various properties, parameters and doneness criteria, other meats (and foods or materials) can be treated using the same model.

For convenience and efficiency of solution, the roast model is divided in half by an imaginary adiabatic wall at the midplane, a plane of symmetry across which no heat is transferred. In Fig. 1, one of the halves (the other is the mirror image) is subdivided axially into J sections; radially, the cylinder is divided into I concentric annuli (the centermost having no hole). With the specified LOD and W and a characteristic density ρ , one can calculate the actual dimensions and thence the model parameters for a specified number and arrangement of elements.

The temperature at each node point is $T(i,j)$ where $i=1,\dots,I$ denotes the radial locations, and $j=1,\dots,J$ the axial locations. The centermost core temperature is $T(1,J)$. In order to facilitate treatment of the surface heat transfer conditions and nonlinearities, the extreme node points are chosen to be *on* the various surfaces (outer, adiabatic midplane) and axis. The resulting nonuniformity of elements is easily accommodated. (See eq. 14-17).

For each of the $I*J$ rectangular cross-section toroids or "donuts" so formed, an energy balance equation is written in terms of the previous temperatures in and around the node of interest and the new node temperature. A temperature change is the result of an imbalance in the heat flows into and out of the toroid. The solution proceeds by incrementing time. For a radiant oven the outside surfaces transfer heat by radiation and convection, most commonly free convection, although forced convection can be treated. Heat is transferred across the interior

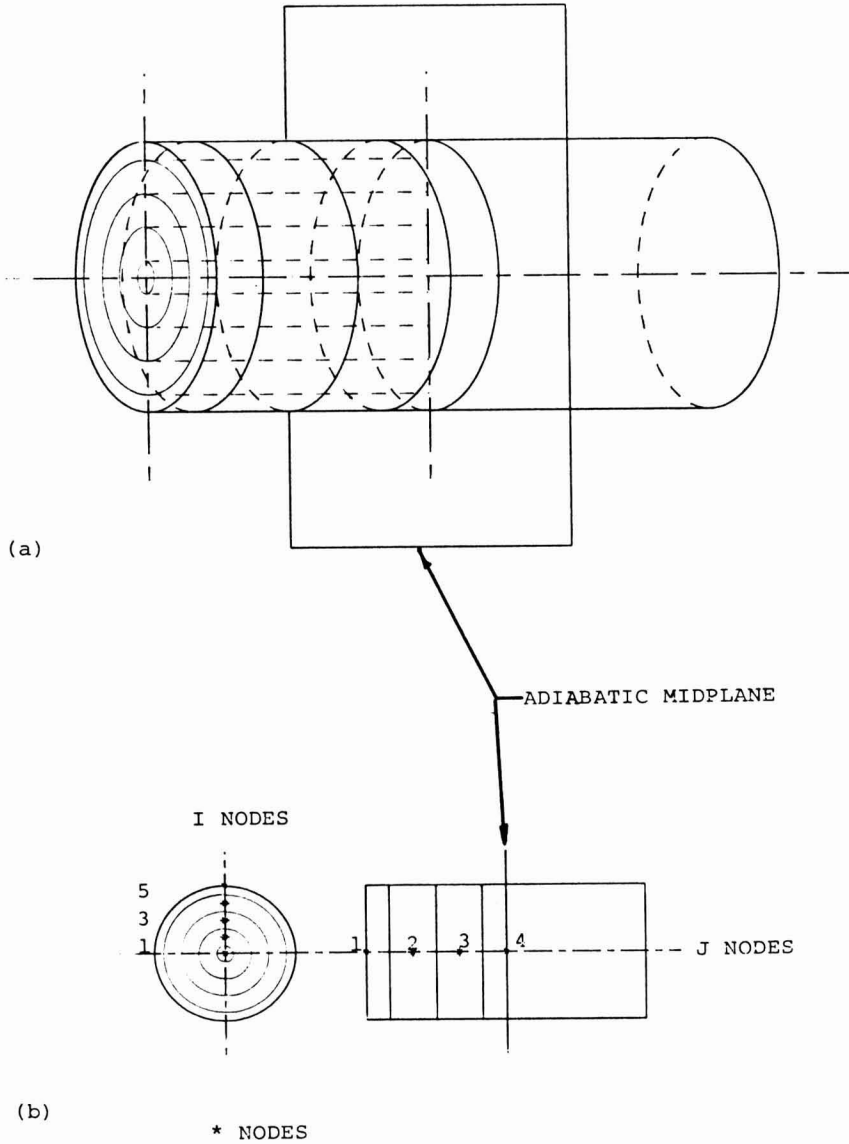


FIG. 1. ROAST MODEL
(a) General view (b) Orthogonal view showing node locations

surfaces by radial and axial conduction, except at the adiabatic midplane. Hence there are six types of elements according to the manner in which heat is transferred across the four surfaces of each toroid; these are identified in Table 2 and in Fig. 1. Except for geometrical considerations, the exterior element types 2,3,4 can be treated identically; the assumed adiabatic surface of element type 4 conducts no heat due to zero temperature difference with the adjacent element due to symmetry; the interior element type 5,6 are likewise similar.

The model takes into account not only heat flows, but possible temperature dependencies of the local properties and latent heats associated with melting and boiling of entrained water. This is done by specifying that property as a function of the local node variables, e.g., temperature, moisture fraction, etc., where the function would be empirical data (tabular) or an equation. The value of the property is computed based upon the values of the variables existing at the present heat transfer calculation. In addition to these temporal considerations as functions of state, spatial variations in the model can take into consideration differences in properties such as the presence of fat or bone and their parametric dependences upon the variables. These are complicating features whose first effect may be to increase the number of elements required of the model, but not necessarily the complexity of the computations or the overall results and conclusions. For the present study, such spatial variations are not included except as functions of local temperatures; if the entire roast is at the same temperature, not the freezing or boiling point, it is assumed to be homogeneous.

The general equation relating heat flows into and out of an element (i,j) is

$$\sum_{n=1}^N q_t(n) = q_s \quad (1)$$

where $q_t(n)$ is the heat transferred across surface n , and N is the number of surfaces. Strictly speaking, each term should be accompanied by an argument (i,j); this is suppressed unless needed for clarity. For the toroidal model here, $N = 4$; heat transfer is axial and radial. For a general case, as with local dissimilar elements, $N = 6$ to allow for tangential heat transfer. Thus, in the form actually used, for a time interval $d\theta$

$$d\theta \sum_{n=1}^4 q_t(n) = q_s d\theta = Q_s \quad (2)$$

The heat stored Q_s in (i,j) is composed of two terms, i.e.

$$Q_s = Q_m + Q_\ell \quad (3)$$

Q_m is the heat required to raise the element temperature by ΔT ,

$$Q_m = mc_p \Delta T. \quad (4)$$

TABLE 2.
CHARACTERIZATION OF ELEMENTS IN MODEL BY MODE OF HEAT TRANSFER ACROSS SURFACES

Number (Figure 3)	Name	Number of Elements in Model*	Exterior Radiant + Convection		Interior Conduction		Adiabatic (No axial conduction)
			Axial	Radial	Axial	Radial	
<u>1</u>	exterior corner	1	1	1	1	1	
<u>2</u>	exterior midplane	1		1	1	1	1
<u>3</u>	exterior end	I-1	1		1	2	
<u>4</u>	exterior diameter	J-1	0	1	2	1	
<u>5</u>	interior midplane	I-1	X	X	1	2	1
<u>6</u>	interior general	(I-2)(J-1)+1	X	X	2	2	0

*where

I = number of axial nodes

J = number of radial nodes

In eq. (3,4) all terms except $d\theta$ are functions of (i,j) . For example, as discussed earlier, c_p may be a function of location and local temperature, i.e., $c_p(i,j,T(i,j))$.

Q_ℓ is the latent heat (function) associated with a change of phase of the fluid in an element at the melting and boiling points only, at which temperatures (specified) the element does not change temperature: $T = Q_m = 0$. Actually, there may be a temperature change, but it will be small. For purposes of computing the heat balance, assuming a constant phase change temperature is inconsequential and greatly facilitates the modeling. Accordingly, Q_ℓ is given by

$$Q_\ell = (L_f \text{ or } L_v)\hat{m} \quad (5)$$

where $\hat{m} = m(i,j) * (\% \text{ water}) * f(T,\theta) \triangleq \hat{m}(T(i,j), \theta(i,j))$. $\hat{m}(T)$ is the mass of the respective remaining (solid or liquid) phase in the element. The function $f(T,\theta)$ can be a complex function which depends upon the temperature-time history and local properties of the roast. During melting, the mass is transformed but not driven off, so m and m of each element will not change. During boiling, moisture can be driven out of an element according to the net heat added to the element, so both m and m will change. If this occurs in an interior element, a mass balance between adjacent elements is needed. However, it is observed computationally (and for a roast to be edible) that for the specified donenesses (including well done), boiling is confined to the exterior (hottest) elements and that moisture is never completely removed from these elements. (For other applications, interior phase changes and mass transfer can be accommodated). Upon recooling, no latent heat of vaporization is involved since the moisture has been driven off; the latent heat of fusion (if refreezing) depends only upon the remaining m . Practically, refreezing is never encountered. Accordingly, Q_s which includes Eq. (3-5) and $f(T,\theta)$ will be a function of the type shown in Fig. 2. Note that over any time increment, $Q_\ell \leq Q_s$, and cumulative values must be accounted for. Q_ℓ is essentially comprised of two impulses whose strengths are proportional to L_f and L_v , occurring at the melting and boiling points, respectively.

Moisture can also be transferred between elements by diffusion, the driving potential being due to the surface evaporation, calculated as above, and thermal gradients. However, since fluid loss is determined by the surface loss, the overall internal effect can be immediately estimated. At least for practical cases, it was observed above that boiling is confined to the extreme outer layer. In addition, there is a steep temperature gradient only at the surface, so that in general the internal concentrations will change relatively slight, although worst case values can be calculated. However, the main effect would be upon the values of the parameters of the elements. Since these dependencies are not fully known, they would appear to be negligible for small changes in concentrations, and this

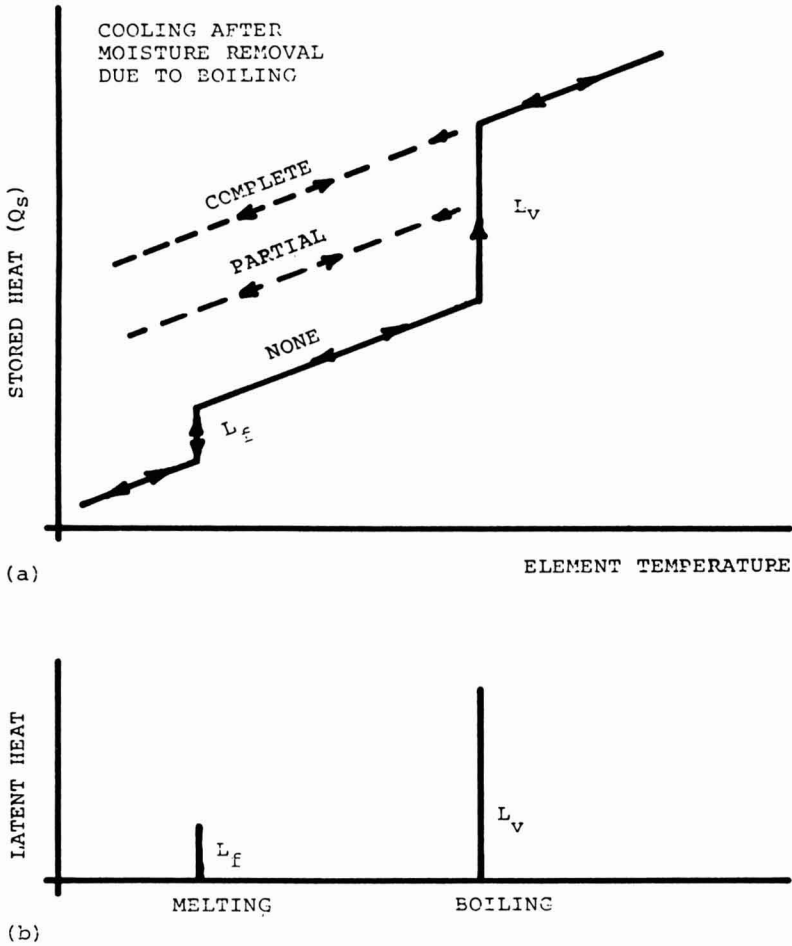


FIG. 2. HEAT CAPACITY FUNCTIONS FOR A TYPICAL ELEMENT, PER UNIT MASS
 (a) Total heat stored (b) Latent heat

aspect is not included in the model. It should be noted that surface desiccation can influence the rate of browning reactions (charring of proteins, etc.), hence the doneness of the roast. These effects could warrant inclusion in future studies and could easily be superimposed, since the form of the equation is the same as the conduction heat transfer equation, Eq. (6) below.

Heat exchange between general interior elements is by conduction only

$$q_k = kA_x \frac{\partial T}{\partial x} \tag{6}$$

where A_x is the area available for conduction (normal to the x-direction), and $\partial T/\partial x$ is the gradient in the x-direction (axial or radial). The temperature gradient is computed across each face of element (i,j) by the temperature difference between the adjacent elements and $T(i,j)$ divided by the distance between the nodes. If q_k is positive for an element (i,j), heat flows 'in' and vice versa, so the convention of Eq. (1,2) follows. Due to symmetry at the adiabatic midplane, Eq. (6) also computes the required zero heat transfer across this axial surface.

The elements on the surface of the roast can lose or gain heat through radial or axial conduction to adjacent interior elements. The outer surfaces of the exterior elements also gain or lose heat through interaction with the oven or other ambient environments by convection and radiation. The general relation for convective heat transfer across the roast surface is

$$q_c = h A_x (T_x - T(i, j)) \quad (7)$$

The surface heat transfer coefficient h depends upon the surface temperature, orientation of the cylinder and specific ambient conditions. In this study we are considering free convection for which h is defined by

$$h = \frac{Nu k_a}{D} \quad (8)$$

The Nusselt number Nu depends upon the orientation of the roast in the oven, for which two cases are practical:

(i) vertical (standing on flat end)

$$Nu = .40 (GrPr)^{1/4} \quad (9)$$

(ii) horizontal (laying on side)

$$Nu = .525 (GrPr)^{1/4} \quad (10)$$

(Rohsenow and Choi 1961; Kreith 1973; Bird *et al.* 1960), where

$$Gr Pr = \left(\frac{D^3 \rho_a g}{\mu_a} \left| \frac{T_\infty - T(i, j)}{T_a} \right| \right) \left(\frac{c_{pa}}{k_a} \right) \quad (11)$$

In Eq. (8-11) k_a , ρ_a , μ_a and c_{pa} are the respective properties of the fluid (air) at the film temperature adjacent to the surface element (i,j), and

$$T_a = \frac{T_\infty + T(i, j)}{2} \quad (12)$$

T_a must be in °R or °K. Forced convection can be treated either by explicit choice of h or some set of empirical relations equivalent to Eq. (8-12).

Heat transfer rate to/from the roast surface by radiation is given by

$$q_r = (\alpha \text{ or } \epsilon) J_x A_x (T_\infty^4 - T(i, j)^4) \quad (13)$$

The so-called view factor J_x for radiation is taken to be unity because the oven sees the full surface area of the roast; the same is assumed for cooling.

Microwaving is easily addressed by including in Eq. (1,2) a microwave energy input term for each volume, proportional to the volume; any attenuation is easily addressed by consideration of geometry. The rest of the solution proceeds without change, modified only by the absence/presence of conventional oven effects.

With specification of the various surface areas and element masses, the model is complete. With the extreme nodal points on the surfaces of the roast, along the axis and in the adiabatic plane, the outer and inner toroids are of radial thickness $\frac{1}{2} dr$, where

$$dr = \frac{D}{2(I-1)} \quad (14)$$

The remaining (I-2) toroids are of radial thickness dr . Similarly, the outer and midplane discs are of axial thickness $\frac{1}{2} dz$, where

$$dx = \frac{L}{2(J-1)} \quad (15)$$

the remaining (J-2) elements are dz thick. Thus, for element (i,j) with the associated outer and inner radii, $r_o(i,j)$ and $r_i(i,j)$, the respective areas A_x across which heat is transferred are

$$\begin{aligned} \text{axial:} & \quad A_x(i,j) = \pi(r_o^2(i,j) - r_i^2(i,j)) \\ \text{radial, outer:} & \quad A_o(i,j) = 2\pi r_o(i,j) * dx(i,j) \\ \text{radial, inner:} & \quad A_i(i,j) = 2\pi r_i(i,j) * dx(i,j) \end{aligned} \quad (16)$$

Finally, the mass of the torodial element (i,j) is

$$m(i,j) = \rho(i,j) * A_x(i,j) * dx(i,j) \quad (17)$$

Computational Considerations

The general computation merely entails applying the appropriate Eq. of (1) – (13) for the parameters associated with each element (i,j) in a marching procedure. This can be easily illustrated using heating as an example. Starting with an initial roast temperature profile (e.g., constant temperature throughout), the roast is introduced into the oven (or other) environment by specification of T_∞ . During the initial time increment, heat is transferred to all peripheral elements by convection and radiation; heat transfer between interior elements by conduction may also occur if the roast begins with a non-equilibrium temperature

distribution. The temperature changes in these elements is calculated according to Eq. (1) – (5). For example, for surface element (i,j) not at a phase-change point.

$$\Delta T = \frac{Q_s}{m c_p} \quad (18)$$

During subsequent time increments, heat is conducted radially and axially, with the rate of conduction being governed by the existing temperature gradients between adjacent elements. Concurrently, heat is added to the peripheral elements (cooking) as in the first time step in accordance with the governing equations for radiation and convection and their newly-established temperatures. An element (node) will change temperature when the net heat flow into an element is not balanced by the heat outflow plus latent heat at a phase change temperature, i.e.,

$$\Delta T = \frac{Q_s - Q_\ell}{m c_p} \quad (19)$$

In Eq. (19) Q_ℓ obeys the “laws” defined in the below Eq. (5) and Fig. 2: active only at a phase change temperature, when the total stored heat $Q_s > 0$, and acting upon and limited by the remaining moisture such that latent heat absorbed $\leq Q_s$. Hence, an element temperature may increase, decrease or stay constant, depending only upon the value of Q_s and whether or not the element is at one of the critical temperatures.

These equations are solved for each element sequentially. Thus, for the initial time increments, the interior-most elements may be unaffected when starting with a uniform internal temperature profile. This marching (through time) procedure is repeated in small evenly-spaced increments until the desired cooking time and/or roast interior temperature is achieved. Changes in the environmental temperature T° can be made at any time (usually preselected). Consequently, multi-stage cooking strategies or cooking followed by setting out at room temperature can easily be implemented.

MODEL PARAMETERS

The roast is assumed to be 60% saline water by weight. For cooking (Guyton 1971), the main effect is on the boiling point; the melting point is relatively less important, as long as it is reasonably low. Where appropriate, the parameters are representative of water. British units are used for convenience. Nominal values of the parameters for beef roast are based on (Rohsenow and Choi 1961), except as noted:

density, ρ	80 lb/ft ³
specific heat, c_p	1.0 BTU/lb °F
thermal conductivity, k	.4 BTU/h ft °F
heat transfer coefficient, h	4 BTU/h ft ² °F (nominal)
absorptivity, δ	.9 (Kreith 1973)
emissivity, ϵ	.9 (Kreith 1973)

As mentioned earlier, the coefficients of radiation absorptivity and emissivity are assumed to be essentially equal; the above value is based on black paint, cf. (Kreith 1973). In the results, the effect of radiation is considered.

From the literature, there is a range of values for these parameters, and while the above may not be the best values available, they are in the ballpark. The doneness at a point in the roast can be expressed in terms of the highest meat temperature achieved at that point, and there is fairly good agreement on these values, per Table 1. In this paper we are primarily interested in doneness at the roast center.

Testing the Model

A trade-off is always involved in terms of computational effort and accuracy. In implementing the computational procedure, we must ensure the stability criteria for the time and spatial intervals are satisfied, e.g. (Kreith 1973 p. 194).

$$d\theta \leq \min \left\{ \frac{(dx)^2 \rho c_p}{2k} \right\} \quad (20)$$

where dx is the smallest spatial increment involved.

Several tests were made of the model, first to check its "accuracy" on simpler problems and to determine a reasonable number of elements, and secondly to identify any particularly salient characteristics or pathologies that might be expected to appear in the remaining studies. As a consequence, it was observed that good accuracy, stability and reasonable computational effort resulted with five radial segments ($I=5$), four axial divisions ($J=4$), 20 elements in all for *half* the roast, and $d\theta \leq .01$ h. It was found that the incremental changes in the results become negligible for increased number of elements or for shorter time increments. It was observed that even for a well done axial midplane node (170 °F) and virtually any reasonable arbitrary oven temperature (550 °F maximum) that only the outer layer of elements ever reached the vaporization temperature. They nearly always achieved it for high enough T_∞ , but never was all the water vaporized, for a practical case.

The program was also used for thawing, which provided a check on the latent heat calculations, viz. elements would remain at the melting temperature until a sufficient quantity of heat was added to accomplish the phase change.

The model was tested for reasonable axial and radial performance by comparing the computer outputs with Heisler chart predictions, e.g. (Newman 1936 pp. 170, 171). Radiation effects (coefficients) are zero for these tests (only). For nondimensionalizing, we use

$$\text{thermal diffusivity, } a = \frac{k}{\rho c_p} = .005 \text{ (all cases)}$$

$$\text{dimensionless time, } = \frac{a\theta}{b^2}$$

$$\text{Nusselt number, } Nu = \frac{hb}{k_a}$$

$$\text{dimensionless temperature, } Y = \frac{T(\theta) - T_\infty}{T_i - T_\infty}$$

In the above, b is half the critical (smallest) overall dimension. T_∞ is the fluid temperature, here 150 °F, and T_i is the initial roast temperature, here 40 °F, to avoid the phase-change considerations.

First, a very flat (steak-like) roast was tested, so that radial conduction effects would be negligible. The resulting centerline temperature was nondimensionalized and compared with that predicted by Heisler charts for a comparably thick infinite slab. For a "roast" of $D = 2$ ft, $L = 2$ in. and cooked for 5.5 h, $\theta = 4$, and $Nu^{-1} = 1.2$ (since $2b = .1667$ ft). For an infinite slab thickness of 2 in., the Heisler charts show a dimensionless temperature $Y = 0.085$. The core temperature predicted by the model was 141 °F, or nondimensionalizing, .0818. Note this is a lower number, representing a higher temperature than that predicted for the infinite slab. This is to be expected, since some heat enters the roast radially.

To test the radial conduction, a long cylindrical roast was utilized, viz. $D = 2$ in., $L = 1.6$ ft, and cooked for 5.5 h. As above $\theta = 4$, and $Nu^{-1} = 1.2$. Using the Heisler charts for an infinite cylinder, $Y = .0052$. The roast model predicts a core temperature of 149.4 °F, or $Y = .005136$. Again, a lower number is obtained, representing a higher temperature due to axial conduction.

RESULTS

The purpose of these results is to demonstrate the model and to address the effects of shape, mass, initial temperature and parameters. A simple cookbook recommendation is included for elementary comparisons. In the cooking tests, the surface heat transfer coefficient and moisture content were allowed to vary, as described earlier. In general, thermal conductivity and radiation coefficients were constant. In (Townsend *et al.*), we shall seek optimal cooking strategies to achieve given doneness profiles.

ROASTING

We “cooked” roasts ranging in weight from 1–10 pounds and length over diameter ratios (LOD) from 0.25 to 4.0. Normally, for $LOD \geq 0.5$, the roast would be on its side, and for $LOD \leq 1.0$, on its end. For $LOD = 0.5$ to 1.0 both orientations are feasible. The most typical roasts were considered to fall in the range of 4 to 8 lb. and LOD of around 1.0. However, many pot roasts are on the order to $LOD = .25$, and the Delmonico is nominally about 2.0.

Cookbook Roasting

The first set of tests involved simply cooking at 350 °F a roast initially at room temperature (70 °F) throughout until the center reached a specified temperature corresponding to the desired doneness. Table 3 shows results of cooking a 5.6 lb. roast (a reasonably common size) to varying donenesses as a function of LOD. Also shown are the recommendations from (Crocker 1969) Table 4 shows results for cooking a range of roast weights and LODs to a rare center. These tables illustrate the results and trends found for other sizes, donenesses, and cooking temperatures. Figure 3 shows a typical result (and the effect of after-cooking, discussed later).

It is clear that the cooking times vary substantially as a function of both weight and LOD, and that simple time per pound rules should be tempered considerably by both the weight and LOD. In all cases, the longest cooking times per pound are for $LOD = 1$. It is easily shown that for a cylindrical shape, the surface-to-volume ratio is least for $LOD = 1$ for a given volume (hence, weight) and increases for both higher and lower values. The surface area governs the rate at which heat can flow into the roast, while the volume dictates the total amount of heat necessary to cook it. Thus, theoretically, the longest time should be for $LOD = 1$; however, the observed longest time may differ slightly from the value due to the surface heat transfer coefficient dependencies on temperature. The maximum times occurred for LOD slightly below 1.0 (about .95). Also, as

TABLE 3.
EFFECT OF LOD AND ORIENTATION ON COOKING TIME TO VARIOUS DONENESSES.
Example: Weight = 5.6 lb.

LOD	Cooking Time, Hours (minutes/lb)		
	Rare 140°F	Medium 160°F	Well 170°F
.25*	1.07 (11.5)	1.33 (14.2)	1.47 (15.8)
.5*	1.73 (18.5)	2.06 (22.1)	2.24 (24.0)
.5	1.67 (17.9)	1.99 (21.3)	2.17 (23.2)
1.0*	1.97 (21.1)	2.33 (25.)	2.54 (27.2)
1.0	1.92 (20.6)	2.27 (24.3)	2.48 (26.6)
2.0	1.52 (16.3)	1.82 (19.5)	1.99 (21.3)
4.0	1.07 (11.5)	1.28 (13.7)	1.40 (15.0)
Rec'd [2]	18-20	20-22	22-24

*vertical roast

would be expected, cooking times are least for the extremes, i.e., for very flat steak-like roasts and long sausage-like roasts. Thus, for the same cooking rule, these would tend to overdoneness; conversely, for LOD = 1, the outcome would tend to be rarer than expected. This is seen in Table 5, which shows the axial doneness profile for a range of roasts and LODS when cooked at 350 °F for a typical length of time rule, viz. 20 min/lb for a rare center. (The trends are significant, not the precise number. In the "Parametric Effects" section, the time dependencies on values of the parameters are discussed.) Except for LOD = 1, there is a strong tendency to overdoneness. For the smaller roasts, LOD = 1 gives over-rare centers, but the larger roasts tend to overdoneness for all LODs.

For a given LOD, the cooking time per pound decreases with increasing weight (Table 4). A 1 lb roast is probably absurd, but the trend is pervasive: in the mid-range LODs, there is a 4 to 5 min per pound decrease in cooking time from, say, a 4-8 lb roast for a given doneness. (Obviously, cooking times increase with doneness, and the results are about proportional.) This occurs because, for a given LOD, the surface area increases more rapidly than the volume.

TABLE 4.
COOKING TIMES TO RARE FOR VARIOUS WEIGHTS AND LODs

Initial Roast Temperature = 70°F
Oven Roast Temperature = 350°F

LOD	Time: Hours (minutes/lb)						
	1	2.2	4.4	5.6	7.8	10.	
.25*	.49 (29.4)	.70 (19.1)	.96 (13.1)	1.07 (11.4)	1.25 (9.6)	-	
.5*	.71 (42.6)	1.06 (28.9)	1.52 (20.7)	1.73 (18.6)	2.06 (15.8)	-	
.5	.68 (40.8)	1.02 (27.8)	1.47 (20.0)	1.67 (17.9)	1.99 (15.3)	1.34 (8.04)	
1.0*	.78 (46.8)	1.19 (32.5)	1.73 (23.6)	1.97 (21.1)	2.38 (18.3)	-	
1.0	.75 (45.)	1.14 (31.1)	1.67 (22.8)	1.92 (20.6)	2.31 (17.7)	2.67 (16.0)	
2.0	.62 (37.2)	.93 (25.4)	1.34 (18.3)	1.52 (16.3)	1.82 (14.0)	2.09 (12.5)	
4.0	.45 (27.0)	.66 (18.0)	.94 (12.8)	1.07 (11.5)	1.27 (9.8)	1.45 (8.7)	

*flat side down
Recommended 18-20 min/lb.

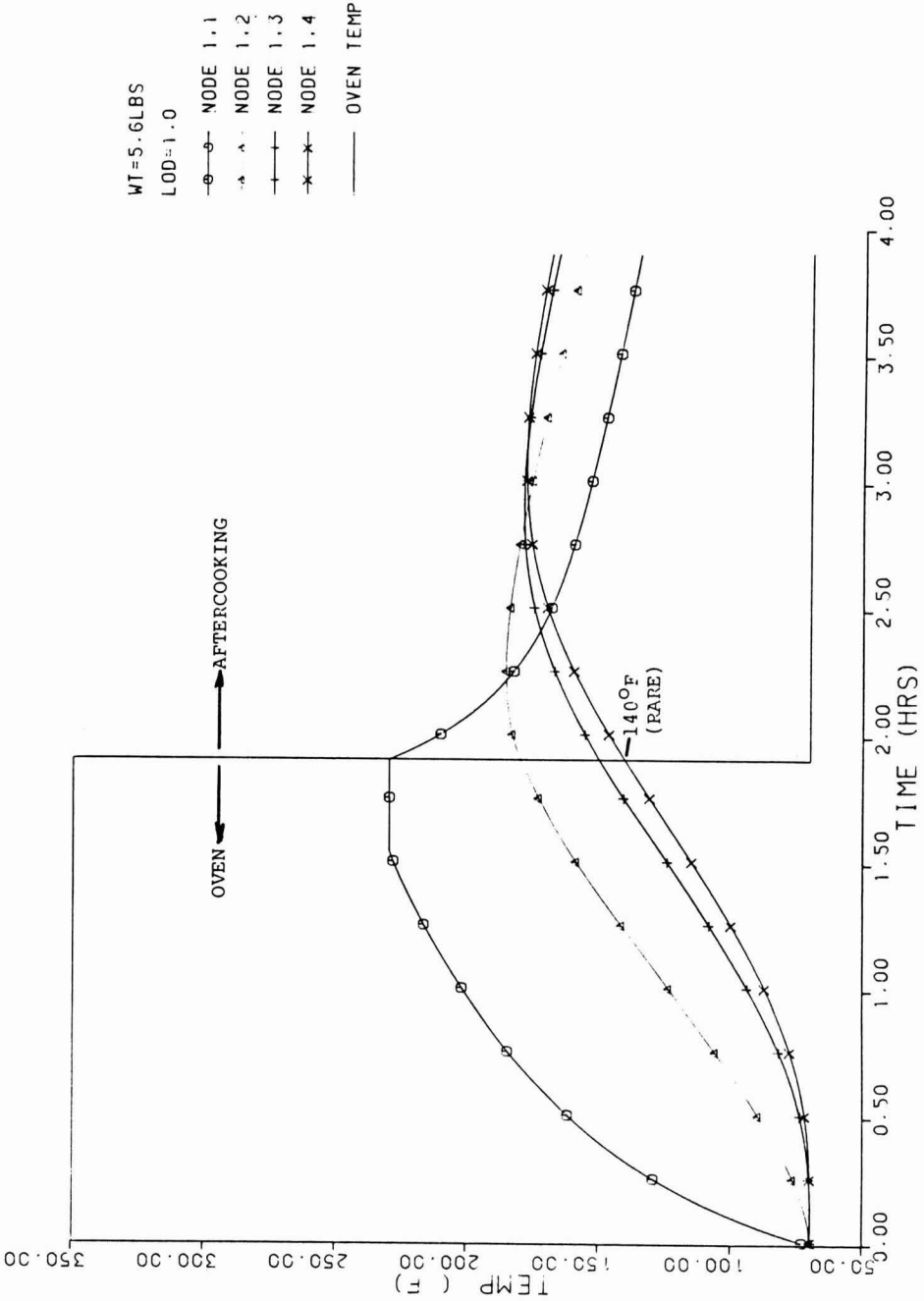


FIG. 3. COOKING TO A 5.6 lb. ROAST, LOD = 1, INITIALLY AT 70°F THROUGHOUT IN A 350°F OVEN UNTIL THE CENTER IS RARE (140°F) Aftercook at room temperature.

There is a insignificant difference in cooking times associated with orientation in the oven, cf. Tables, 3,4. Cooking time is always slightly less with the cylindrical axis horizontal, due to the small difference in the constants in Eq. (9,10).

Per Table 5 and the above discussion, the check out a cooking "law", as Eq. (i) of Klamkin (1962) or Eq. (iv), roasts of weights from 1 to 7.8 lb, all with $LOD = 1$, were cooked at different temperatures until the center was rare (140°F). The results are shown in Fig. 4. This plot gave rise to Eq. (v), viz. cooking time increases at about (mass) .50 to .55. This indicates that surface convection and radiation effects are significant relative to internal conduction effects. Obviously, the time decreases with increasing oven temperature; by cross plotting, the cooking time was about proportional to $(T_{\infty} - T_{DONENESS})^{-2}$. The principal difference is that the doneness of the outer and middle sections, the amount and depth of well-done meat, increases with increasing oven temperature.

From the results for cooking time as a function of LOD (cooking time per lb is a maximum for $LOD = 1$) and Eq. (i)-(iv) if the Introduction, we might expect that the exponent of a cooking time "law" would increase for LODs greater and less than 1. That is, as the surface area/volume ratio increases, presumably conduction would tend to dominate, and the exponent would increase. In fact, the opposite happens, although not to any great extent. For $LOD = 2$, the exponent is .50 to .55 for the same over temperatures in Fig. 4; for $LOD = .25$, the exponent is about .45 to .50. The highest exponents also occur for the highest oven temperature. The explanation for this is probably due to the nonuniformity of heating and the doneness criterion of time to a 140°F center: for a long or flat roast, the heat transfer is essentially one-dimensional, whereas for LOD in the range of 1, two-dimensional heat flow is significant.

Effect of Initial Temperature Thawing

Next, trials were conducted to establish the influence of initial roast temperature on the cooking time. (In the above, the initial roast temperature was 70°F throughout.) For a roast which has come directly from the refrigerator an initial profile of 40°F throughout might be expected. For a roast taken directly from freezer to oven, the starting temperature was assumed to be 10°F. The results are shown in Table 6 for several typical roast sizes. The effect of oven thawing can be seen in the simulation of Fig. 5, which also shows aftercooking, discussed below.

The problem of simply thawing at room temperature a roast initially at 10°F was addressed. Table 7 shows thaw times (center temperature exceeding 32°F). As in cooking, there is a considerable variation with LOD, the maximum times occurring at or just below $LOD = 1.0$.

TABLE 5.
ROASTING AT RECOMMENDED TIMES AND TEMPERATURES

Oven temperature = 350 °F
Assumed desired doneness: rare center
Recommended time = 20 minutes/lb.

Cooking Weight, lb	Time, hours	LOD	Doneness Temperature °F			
			J = 1 (outside)	Axial Node J = 2 J = 3		J = 4 (center)
4.4	1.47	.5	223	178	151	141
		1.0	230	168	135	126
		2.0	230	173	154	150
5.6	1.87	.5	230	190	163	154
		1.0	230	178	148	138
		2.0	230	184	167	164
7.8	2.60	.5	230	200	178	171
		1.0	230	189	163	154
		2.0	230	196	182	179

Aftercooking

One interesting aspect involves removing the roast from the oven 'early', allowing further cooking to proceed while the roast sits at room temperature. The roast center continues to cook as the outer, hotter sections lose heat both to the roast center and to the environment. A verification of this phenomenon is seen in Fig. 3 and 5 in the temperature profile at four axial roast locations (outermost, 2 intermediate, centermost) following removal from a 350 °F oven to a 70 ° room. It can be seen that continued center temperature increases occur for some considerable time after removal from the oven, while the outer temperatures decrease. In the optimization study (Townsend *et al.*), this effect may be useful in getting the desired doneness profile.

Parametric Effects

All roasts heretofore discussed have considered radiation effects using an absorptivity of 0.9 (Kreith 1973 for black paint). In order to determine the effects of radiation a number of studies were conducted with lower absorptivities. Values selected included 0.8, 0.4, and 0.0. The last case, of course, is for no radiation effects at all. The results are shown in Table 8. It can be seen that radiation effects are considerable even at the relatively low temperatures involved. The effect is accentuated by the melting phase (cooking from 10 °F).

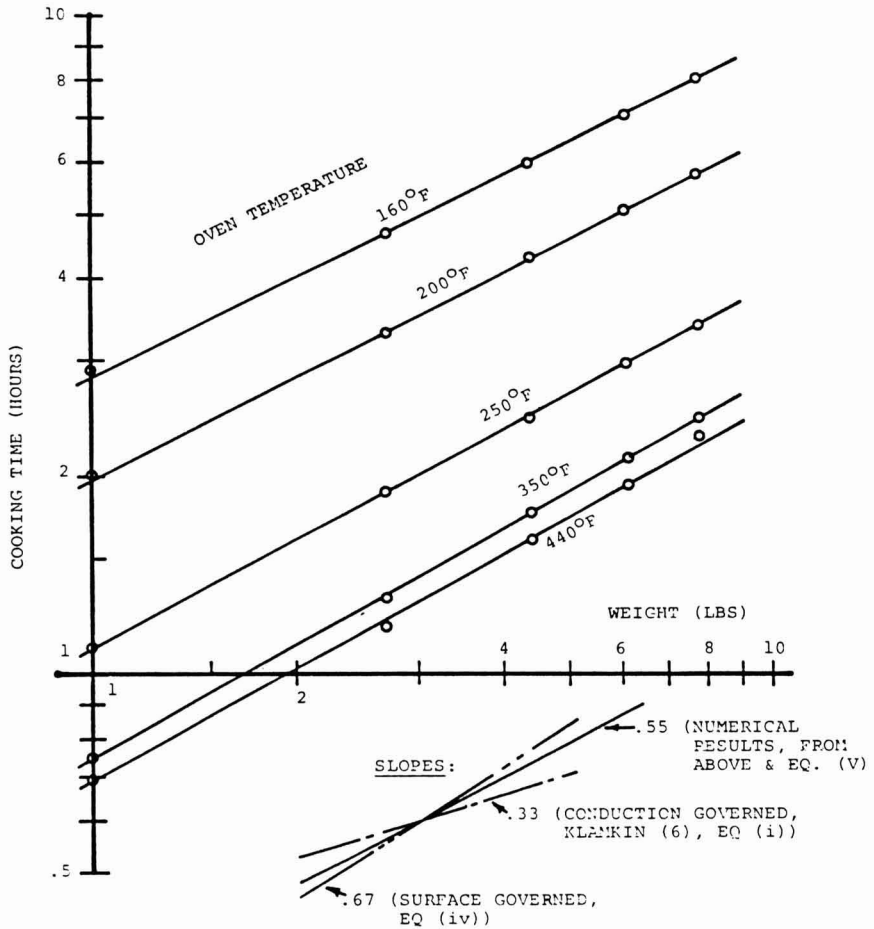


FIG. 4. COOKING "LAW" TESTS FOR LOD = 1.0, RARE CENTER (140°F) ROAST INITIALLY AT 70°F THROUGHOUT

Some tests were run with a thermal conductivity that was decreased by 20% to $K = .32$; typical results are shown in Table 9. As can be seen, this also affects cooking time considerably.

Tests were not run with variable specific heat or density. Clearly, these merely affect the amount of heat absorbed by the body, and both will change cooking time proportionally.

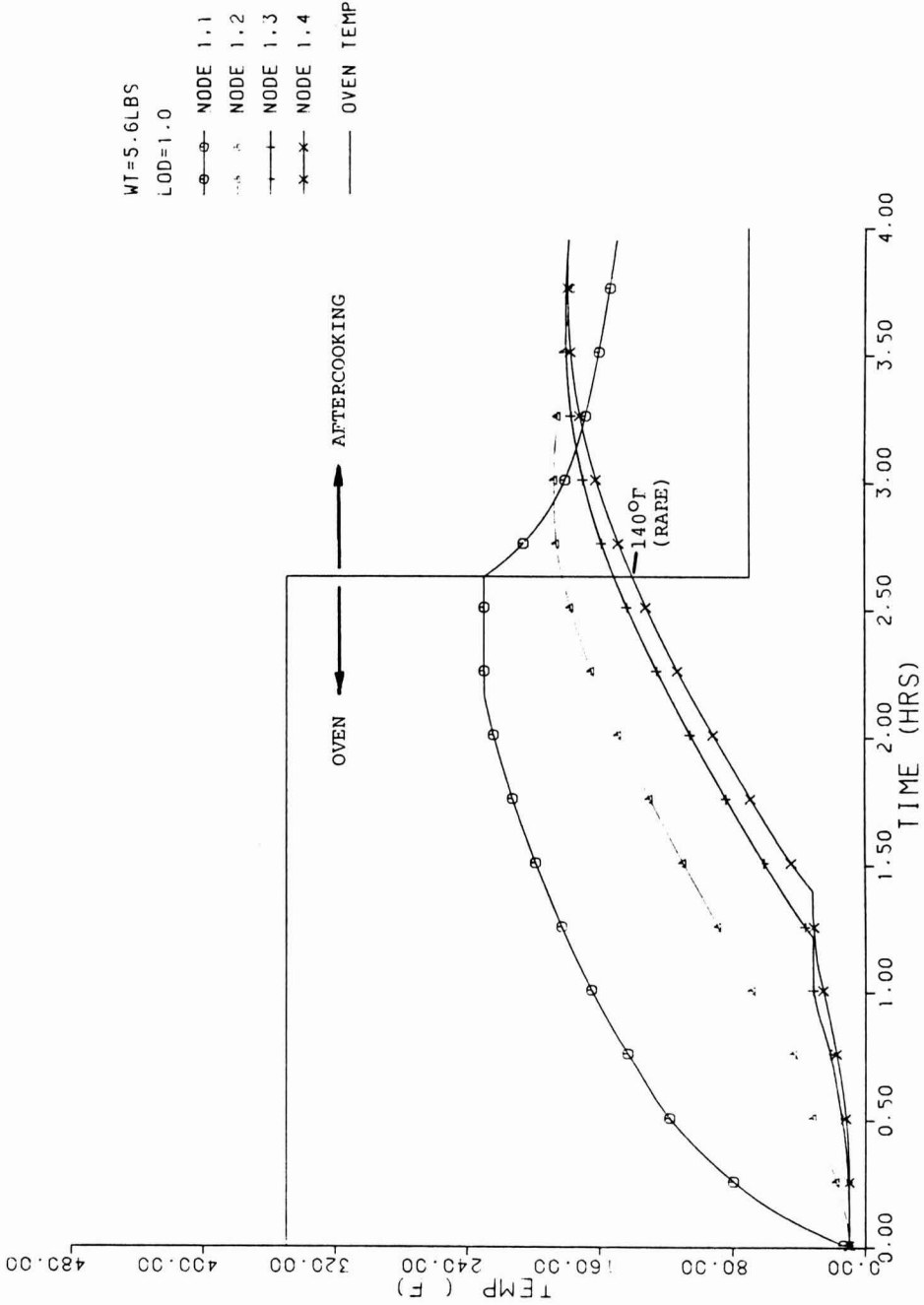


FIG. 5. COOKING OF A 5.6 lb. ROAST, LOD = 1, INITIALLY AT 10°F THROUGHOUT (FROZEN) IN A 350°F OVEN UNTIL THE CENTER IS RARE (140°F).
 Aftercook at room temperature.

TABLE 6.
EFFECT OF INITIAL TEMPERATURE ON ROASTING TIME

Initial Roast Temperature		Roasting Time, Hours (minutes/lb)		
		Room 70°F	Refrigerated 40°F	Freezer 10°F
Weight, lb	LOD			
	4.4	.5 1.47 (20.0)	1.75 (23.9)	2.13 (29.0)
		1.0 1.67 (22.8)	1.97 (26.9)	2.36 (32.2)
	2.0 1.34 (18.3)	1.60 (21.8)	1.92 (26.2)	
5.6	.5	1.67 (17.9)	1.99 (21.3)	2.40 (25.7)
	1.0	1.92 (20.6)	2.25 (24.1)	2.64 (28.3)
	2.0	1.52 (16.3)	1.82 (19.5)	2.17 (23.2)

TABLE 7.
HEATING FROM 10°F TO 35°F (AT CORE) AT ROOM TEMPERATURE (70°F)

Weight lb	Time (Hours)				
	LOD				
	.25	.5	1.0	2.0	4.0
1.0	5.5	7.06	7.49	6.66	5.12
2.0	7.84	10.21	11.02	9.9	7.66
4.4	12.4	15.4	16.2	14.36	10.95
5.6	13.91	17.47	18.37	16.21	12.25
7.8	16.12	20.72	22.06	19.41	14.41
10.	18.03	23.39	24.95	22.06	16.43

TABLE 8.
EFFECT OF RADIATION ON COOKING TIME

Cooking time to rare core (140°F) in 350°F oven
5.6 lb. roast, LOD = 1

Absorbitivity	Cooking Time, Hours	
	from 70°F	from 10°F
0.9 (normal)	1.92	2.64
0.8	1.96	2.88
0.6	2.09	2.94
0.4	2.26	3.43
0.2	2.51	3.88
0.0	2.93	4.70

TABLE 9.
EFFECT OF THERMAL CONDUCTIVITY (k) ON COOKING TIME

Cook to rare in 350°F oven
Roast initial temperature = 70°F
LOD = 1

Weight, lb	Cooking Time, Hours	
	k = .4	k = .32
1	.78	.85
2.2	1.14	-
2.7	-	1.48
4.4	1.67	1.95
5.6	1.92	2.24
7.8	2.31	2.73

CONCLUSIONS

In modeling the roast process, it has been seen that cooking time recommendations for a given doneness should be predicted on more than weight. Aftercooking at room temperature for even a short time can significantly increase the interior doneness. Even for a roast well done at the center, boiling and moisture loss occur only at the surface, and the outer surface never exceeds the boiling

temperature. In the model, moisture loss of the outer elements never exceeded 50%. The defrosting process as well as cooking a frozen roast have been demonstrated. The model was validated against classical infinite boundary solutions, showing slightly higher core temperature for a given time, as expected due to transverse heat conduction and heat entering through the finite ends of the roast.

After considering possible competing cooking "laws", plotting results indicate that cooking time is proportional to (weight, or mass)^{0.55} for a given family of similar roasts cooked from the same initial temperature to the same core doneness. Similarly, the cooking time is about proportional to $(T_{\infty} - T_{\text{DONENESS}})^{-2}$.

A companion paper (Townsend *et al.*) considers the optimization of the cooking process.

NOTATION

A_s	surface area
A_x	surface area in direction of conduction (x)
c_p	specific heat
D	roast diameter
$dz, dz(i,j)$	thickness of axial slices, slice (i,j)
h	surface heat transfer coefficient
i, I	radial sections (index)
j, J	axial sections (index)
J_x	view factor for radiation
k	thermal conductivity
L	roast length
L_f	latent heat of fusion
L_v	latent heat of vaporization
LOD	length over diameter ratio
m	mass of an element
m	mass of water in an element
Nu	Nusselt number (see Eq. 8-12)
q_{in}, \dot{q}_{in}	input heat, heat rate
q_k	heat conduction rate
q_s	heat stored (rate) in an element
$q_t(n)$	heat transfer through surface n of an element
Q_ℓ	latent heat function
Q_m	capacitive heat in an element
Q_s	quantity of heat stored in an element

$r_o(i,j)$	outer radius of element i,j
$T(i,j)$	node temperature in segment i,j
T	oven (ambient) temperature
W	roast weight

Greek Symbols

α	surface absorbtivity
ϵ	surface emissivity
θ	time
θ_c	cooking time
μ	viscosity
ρ	density

REFERENCES

- Better Homes and Gardens Editors. 1959. *Meat Cook Book*, Meredith Publishing Co., New York.
- BIRD, R.B., STEWART, W.E. and LIGHTFOOT, E.N. 1960. *Transport Phenomena*, John Wiley & Sons, New York.
- CROCKER, B. 1969. *Betty Crocker's Cookbook*, Golden Press, New York.
- GUYTON, A.C. 1971. *Textbook of Medical Physiology*, p. 380. W.B. Saunders, Philadelphia.
- KLAMKIN, M. 1962. On cooking a roast. *SIAM Review*, 3, (2), 167-169.
- KREITH, F. 1973. *Principles of Heat Transfer*, Intext, New York.
- NEWMAN, A.B. 1936. Heating and cooling rectangular and cylindrical solids, *Ind. Eng. Chem.* 28, 545-548.
- ROHSENOW, W.M. and CHOI, H. 1961. *Heat, Mass, and Momentum Transfer*, Prentice-Hall, Englewood Cliffs, New Jersey.
- ROMBAUER, I.S. and BECKER, M.B. 1973. *Joy of Cooking*, Bobbs-Merrill, Indianapolis.
- TOWNSEND, M.A. and GUPTA, S and PITTS, W.H. Optimization of a nonlinear multiple-stage heat treatment problem: the roast (II).

A FINITE ELEMENT METHOD TO MODEL STEAM INFUSION HEAT TRANSFER TO A FREE FALLING FILM

KATHRYN L. MCCARTHY¹

*University of California, Davis
Davis, California 95616*

and

RICHARD L. MERSON

*University of California, Davis
Davis, California 95616*

Accepted for Publication September 23, 1988

ABSTRACT

This work is a theoretical and experimental analysis of heat transfer to a free falling film of homogeneous fluid food. Fluid falls vertically in a thin film through a stagnant steam environment. The thermal energy equation governing the steady state heat transfer is solved numerically by a finite element method. The Froude number and the Peclet number characterize the fluid flow and heat transfer. Water was used as the experimental test fluid in the steam infusion unit. Average fluid temperatures measured as a function of position compare well with model predictions. The model was incorporation into a kinetic model to predict the extent of microbial destruction expected with the time/temperature treatment.

INTRODUCTION

Homogeneous liquid foods may be heated for sterilization as a film falling freely through condensing steam. This steam infusion method has the advantages that heating is rapid and uniform, cooling can be achieved rapidly by flash evaporation of the condensate, and fouling is minimized because there are no heat transfer surfaces. To calculate the degree of sterilization achieved, the film temperature must be known as a function of exposure time.

¹Address correspondence to K.L. McCarthy, Dept. of Food Science and Technology, University of California, Davis, Davis, CA 95616

The velocity profile of a thin free falling film has been studied theoretically and experimentally in connection with curtain coating (Brown 1961). The experimental apparatus formed a thin film of viscous liquid which fell a distance without surface contact and then impinged on a rapidly moving surface. The velocity was measured photographically and an empirical expression deduced to calculate the velocity for viscosities in the range of 1.2 to 9.9 Poise.

The velocity profile and heat transfer to a free falling film were also studied analytically by Murty and Sastri using an integral method (1973, 1974, 1976). Quadratic expressions for the vapor velocity, liquid velocity, and temperature profile were assumed. The expressions were substituted into the integrated partial differential equations for the conservation of mass, momentum, and thermal energy. A parametric analysis correlated the local Nusselt number with the Prandtl number, ratio of Reynolds number to Froude number, and Jakob number. In a related problem, Rao and Smith (1984) studied the condensation of vapor on the surface of a laminar film of immiscible liquid on an inclined plane.

Heat transfer experiments have not been performed previously with free falling films. The objectives of this work are to mathematically model the fluid flow and heat transfer in a thin falling sheet of a homogeneous fluid food and to verify the model experimentally. With the resulting temperature profile for the film and rate kinetics for the destruction of microorganisms, the extent of sterilization is predicted.

MATERIAL AND METHODS

Experimental Apparatus

This work mathematically models and experimentally verifies the velocity and temperature profiles of a film as it falls vertically in a steam chamber. As it falls, the sheet thins due to the acceleration of gravity. Figure 1 illustrates the film. Flow is in the x-direction. The film thickness is measured in the y-direction; the original film thickness is on the order of one millimeter. Film width is measured in the z-direction.

The experimental apparatus consisted of a falling film enclosed in a steam chamber (Fig. 2). Saturated steam at atmospheric pressure entered the chamber through a vertical spreader and was evenly dispersed as it passed through two perforated baffles. Continuous venting through loose fittings proved adequate to maintain atmospheric pressure and to prevent buildup of noncondensable gases.

Water, used as the test fluid, was pumped through a rotameter to the cylindrical reservoir at flow rates from 1.6 L/min to 2.3 L/min. The fluid entered the steam chamber through a slit 7.6×10^{-2} m in width and 8.9×10^{-4} m thick. As the fluid fell, the sheet remained intact with the aid of two guide wires ($1.0 \times$

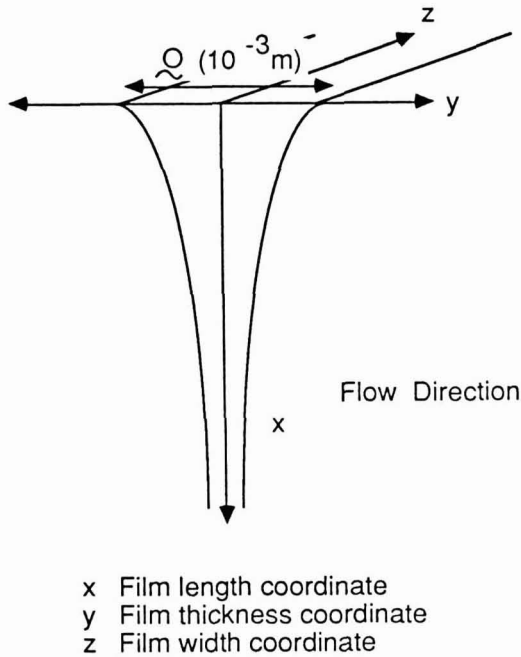


FIG. 1. FILM OF FALLING LIQUID IN A STEAM ENVIRONMENT

10^{-3}m diameter) set $7.6 \times 10^{-2}\text{m}$ apart. Before flowing to the drain, fluid was detained temporarily in a variable height trough in which temperature measurements were taken. The collection trough position was adjustable from film lengths of 1.2×10^{-2} to $1.0 \times 10^{-1}\text{m}$.

Temperature measurements were recorded as a function of film length with 30 gauge copper-constantan thermocouples and a recorder/datalogger (Molytec Recorder/Datalogger, Pittsburg, PA). The temperature of the steam chamber was constant and uniform and one thermocouple measurement proved adequate. Four thermocouples were secured in the adjustable collection trough. Due to the mixing in the trough, these measurements were considered the average temperature at a given film position. The estimated uncertainty in the experimental measurements was $\pm 1^\circ\text{C}$. As the fluid exited the steam chamber, a thermocouple recorded the temperature. Any increase in fluid temperature due to residence time in the drain tube was not measurable.

The axial velocity profile of the film was verified by streak photography. Particles were introduced into the water and photographed as they fell through the chamber. Illumination was provided by a 500 W flood lamp behind the film.

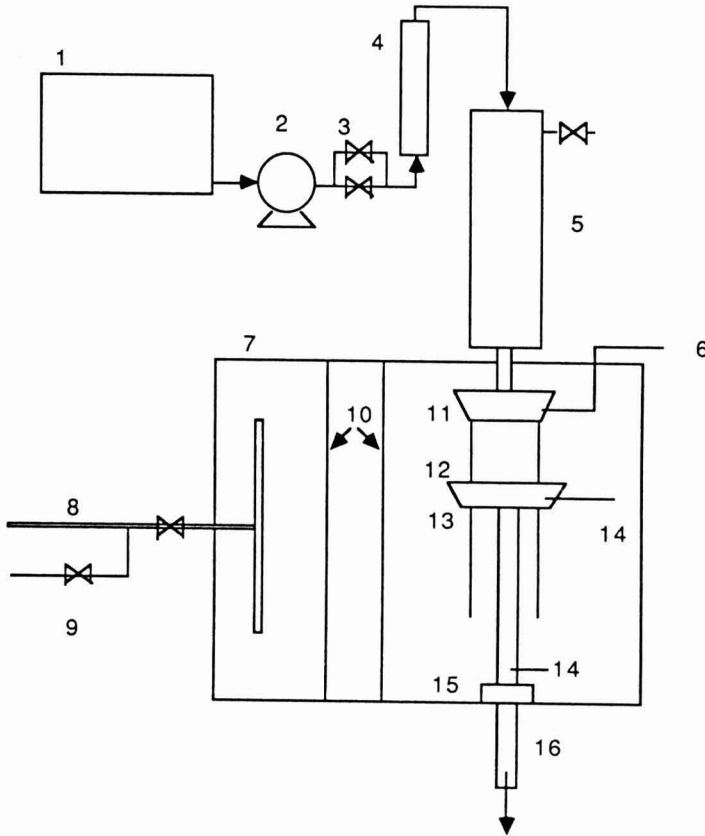


FIG. 2. EXPERIMENTAL APPARATUS

- | | | | |
|--|-----------------------------|------------------------------|---------------------------------|
| 1 . Liquid reservoir with level control | 5 . Constant head reservoir | 10. Baffles | 14. Thermocouples to datalogger |
| 2 . Centrifugal pump with speed controller | 6 . Manometer | 11. Trough with narrow slit | 15. O-ring seals |
| 3 . Bypass and valves | 7 . Steam chamber | 12. Guide wires | 16. To drain |
| 4 . Rotameter | 8 . Steam sparger | 13. Adjustable height trough | |
| | 9 . Condensate drain | | |

Photographs were taken at 1/125 s shutter speed with a tripod-mounted 35 mm camera fitted with a Macro lens. The velocity profile was obtained by measuring the distance the particle fell as a function of position in the film.

Numerical Solution

The following analysis is restricted to a low viscosity Newtonian fluid falling under gravity in laminar flow at steady state. Physical properties are assumed constant. The heating medium is steam with negligible resistance to heat transfer at the film surface. Fluid flow is assumed fully developed so transverse velocity gradients are neglected.

The thermal energy equation and boundary conditions for the free falling film are (McCarthy 1985)

$$\text{PDE } \rho c_p u(x) \partial T / \partial x = k \partial^2 T / \partial y^2 \quad (1)$$

$$\text{BC1 } x = 0 \quad T = T_0 \quad (2)$$

$$\text{BC2 } y = 0 \quad \partial T / \partial y = 0 \quad (3)$$

$$\text{BC3 } y = \delta(x) \quad T = T_{st} \quad (4)$$

The expressions are made dimensionless by

$$x = x/L \quad (5)$$

$$y = y / \delta(x) \quad (6)$$

$$\theta = (T - T_0) / (T_{st} - T_0) \quad (7)$$

When viscous stresses are negligible, as with low viscosity fluids, the velocity profile can be described by (Scriven and Pigford 1959)

$$u(x) = (u_0^2 + 2gx) / 2 \quad (8)$$

The dimensionless variable ψ is introduced to characterize the velocity

$$\psi = 1 + 2gxL / u_0^2 \quad (9)$$

so that

$$u(x) = u_0 \psi^{1/2} \quad (10)$$

By conservation of mass, the half film thickness $\delta(x)$ is

$$\delta(x) = h_0 \psi^{-1/2} \quad (11)$$

Making Eq. (1)–(4) dimensionless by introducing Eq. (5)–(7), (10) and the Peclet number (Pe), Froude number (Fr), and dimensionless length (h_0/L) yields

$$\text{PDE } (Pe/Fr)(h_0/L)y\psi^{-3/2} \partial \theta / \partial y + Pe(h_0/L) \psi^{-1/2} \partial \theta / \partial x = \partial^2 \theta / \partial y^2 \quad (12)$$

$$\text{BC1 } x = 0 \quad \theta = 0 \quad (13)$$

$$\text{BC2 } y = 0 \quad \partial \theta / \partial y = 0 \quad (14)$$

$$\text{BC3 } y = 1 \quad \theta = 1 \quad (15)$$

$$\text{BC4 } x = 1 \quad \partial \theta / \partial x = 0 \quad (16)$$

$$Pe = \rho c_p u_0 h_0 / k \quad (17)$$

$$Fr = u_0^2 / gL \quad (18)$$

$$\psi = 1 + 2x / Fr \quad (19)$$

The fourth boundary condition is added for the finite element formulation; the temperature or flux must be specified on all boundary elements. The length of the film, L , is chosen far enough downstream that axial gradients are negligible.

The partial differential equation was solved by a finite element method (McCarthy 1987) to obtain a temperature map as a function of axial and transverse coordinates as well as average temperature at various distances along the film. The Galerkin method was used: shape functions and weighting functions were bilinear. The elements were isoparametric quadrilaterals. Calculations for the temperature and flux values for the 160 element grid used took approximately two minutes CPU time on a Digital Equipment Microvax II.

RESULTS AND DISCUSSION

Temperature profiles resulting from the numerical solution are functions of the Peclet number and the Froude number. If only one parameter at a time were varied experimentally, the profiles would resemble Fig. 3 and Fig. 4. The dimensionless temperature averaged across the film at a specified x -position is plotted against the dimensionless variable x . In all cases, the characteristic length, L , is the film length that allows the average film temperature to reach within one percent of the steam temperature. Figure 3 illustrates the trend of the temperature profile as the Peclet number increases. The range of Peclet numbers in the figure corresponds to the range for the experimental runs. As the Peclet number increases, the ratio of convection to conduction increases. As the exposure time of the fluid to the steam environment decreases, the average temperature of the film at a given position decreases. In Fig. 4, as the Froude number increases, the ratio of inertial forces relative to gravity forces increases. Again, the average fluid temperature decreases for a given position in the x -direction.

Experimentally the parameters varied were the flow rate and the position of the collection trough. The first experimental measurements (Fig. 5) of the average temperature were made at an initial velocity of 0.39 m/s, corresponding to a Pe of 1160 and a Fr of 0.053. The data points were taken at film lengths from 1.2×10^{-2} to 7.2×10^{-2} m. The average dimensionless film temperature is plotted against the dimensionless distance in the x -direction, made dimensionless with $L = 3.0 \times 10^{-1}$ m. The experimental values compare well with the model-predicted curve within the experimental range.

Increasing the flow rate to an initial velocity out of the slit of 0.47 m/s increased the Peclet number to 1380 and the Froude number to 0.064. Figure 6 illustrates the predicted temperature profile and the measured data points for these parameters. In this case, the distance L was 3.5×10^{-1} m.

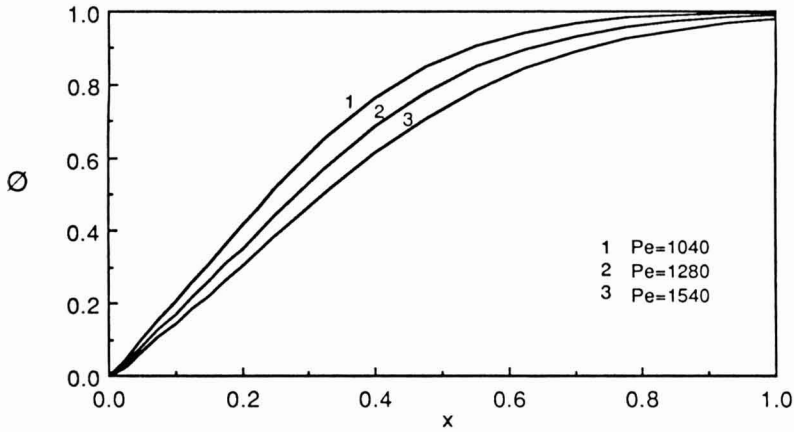


FIG. 3. TEMPERATURE PROFILE AS Pe VARIES

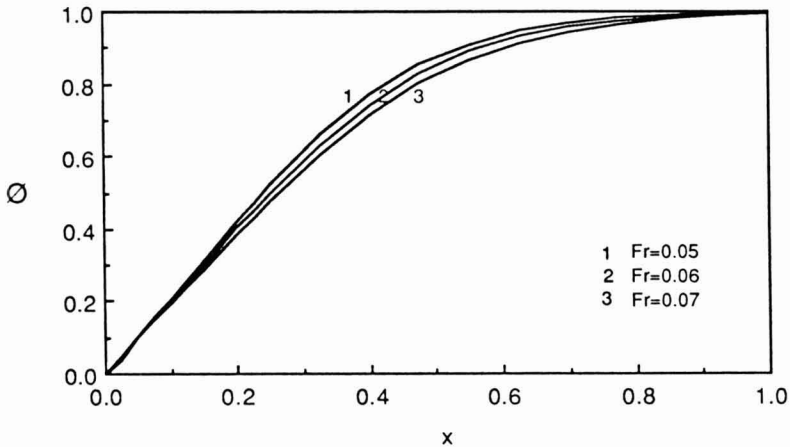


FIG. 4. TEMPERATURE PROFILE AS Fr VARIES

The third set of temperature measurements taken at $u_0 = 0.56$ m/s, $Pe = 1640$, $Fr = 0.070$, and $L = 4.5 \times 10^{-1}$ m is shown in Fig. 7.

Due to the increasing instability of the film in the steam environment, more scatter in the data is observed in Fig. 6 and 7. In falling film applications (fluid flowing along a surface), liquid films are generally not planar. Usually the film is rippled, and under these conditions the mass transfer rate is increased significantly beyond the rate predicted for the theoretical model based on

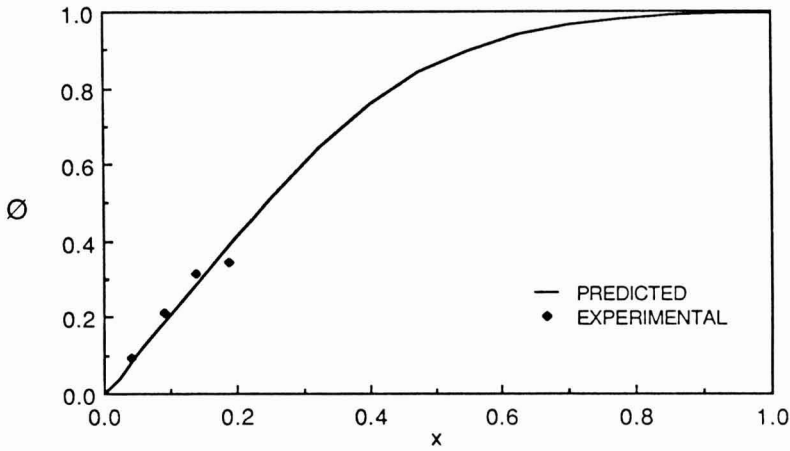


FIG. 5. TEMPERATURE PROFILE: $Pe=1160$, $Fr=0.053$, $h_0/L=0.0015$

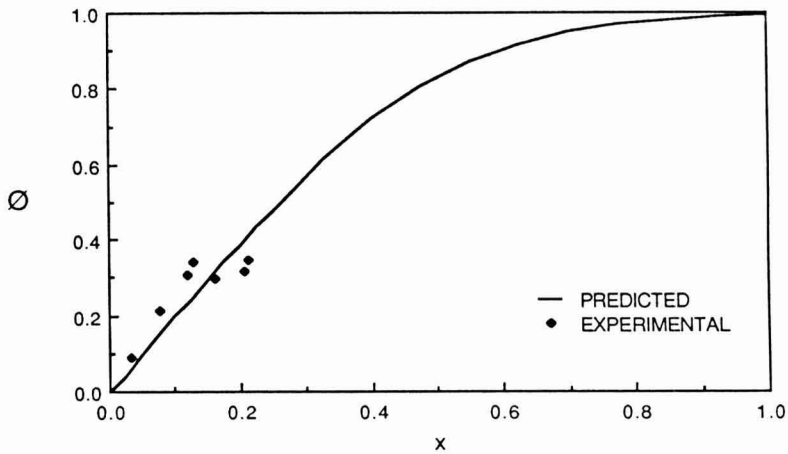


FIG. 6. TEMPERATURE PROFILE: $Pe=1380$, $Fr=0.064$, $h_0/L=0.0013$

laminar flow, due to convection within the film (Barrdahl 1988). The same phenomenon is expected for heat transfer in the free falling film, especially as the flow rate increases. The steeper slope of the data points at lower values of x in Fig. 6 and 7 indicate a greater heat transfer rate than predicted. At higher values of x , the principal cause of instability of a thin liquid sheet is the interaction of the sheet with the surrounding atmosphere. Experimentally, break up occurred beyond film lengths of 7.5×10^{-2} m. Data were not collected after break

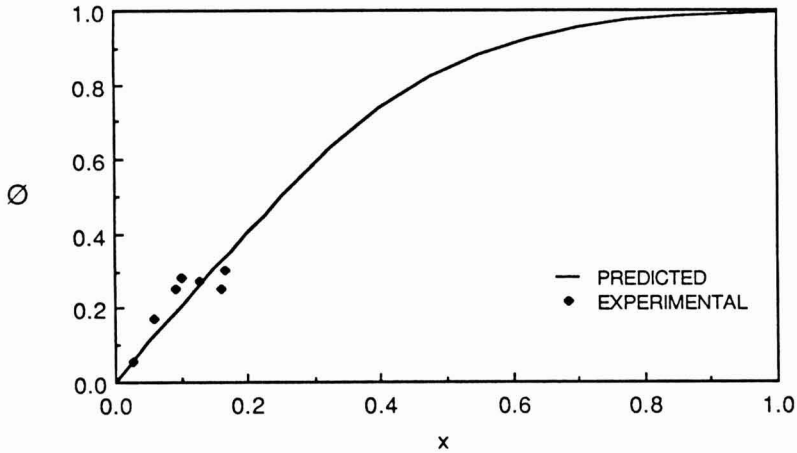


FIG. 7. TEMPERATURE PROFILE: $Pe=1640$, $Fr=0.070$, $h_0/L=0.0010$

up since the objective of this study was to investigate intact liquid sheets. Disintegration of the sheet occurs as rapidly growing waves reach a critical wave amplitude and fragments of the sheet are torn off (Dombrowski and Johns 1963).

The dynamics of thin sheets of liquid have been studied in connection with atomization, spray coating, and curtain coating. Brown (1961) verified the condition for film stability at any point as a balance of inertia forces and surface tension. Linear theory has been used to investigate the stability of falling sheets (Lin 1981; Lin and Roberts 1981). For a viscous liquid flowing vertically between two guide wires, Lin (1981) confirmed theoretically that a stable film could be maintained only if the Weber number, σ/Qu , is less than $1/2$. This predicted critical Weber number agreed with experimental results by Brown (1961). The Weber number in this study ranged from 0.53 at low flow rates to 0.26 at higher flow rates.

The effect of condensate did not appear to be important either as resistance to heat transfer or as increase in mass. Equation (3), which assumes no resistance to heat transfer at the film surface, proved adequate for this range of parameters. The flow rate increased by only 4% as the liquid flowed through the chamber.

The final objective in this study was to insure a commercially sterile product assuming the fluid remains in an intact sheet as it falls through the steam chamber. The following expression yields the exposure time of the liquid to the steam environment at a given location in the direction of flow (McCarthy 1985).

$$t = [(u_0^2 + 2gx)^{1/2} - u_0] / g \quad (20)$$

Sterilization is based on the first order rate kinetics of microbial destruction, where k' is the rate constant.

$$dN/dt = -k' N = -2.303 N / D_T \quad (21)$$

Microbiologists frequently use the D value (D_T) in this relationship. The D value is the time required, at a constant temperature, to destroy 90% of a population of microorganisms present in the food. A thermal process design is based on the required number of decimal reductions, n , of the most heat resistant microorganism likely to be present. The product of this number and the D value is referred to as the F value required for commercial sterilization. Thermal processes are also considered in terms of the time/temperature treatment of the product. Since most thermal processes are not at a constant temperature, the F value for a process is an integral taken over the process time. The integral accounts for the first order rate kinetics of microbial destruction and the temperature dependence of the D value.

$$F_{T_{ref}} = n D_{T_{ref}} = \int_0^t 10^{(T(t) - T_{ref})/z} dt \quad (22)$$

The z value is the temperature change that represents a ten-fold change in the D value.

In practice, all microbial destruction is assumed to take place in the constant temperature holding tube, which follows the heating step. Therefore, the ideal situation is to heat the fluid as rapidly as possible. Calculation of extent of bacterial destruction in the heating portion of the process can be calculated by Eq. (22) using Eq. (20) for the residence time, t . Based on the lowest temperature in the film (along the center line) calculated with the model as the fluid approaches steam temperature, less than 0.1% of the total microbial destruction required for a sterile product occurs during the heating step with this steam infusion method. This calculation is based on the thermal destruction of the microorganism, *Clostridium botulinum* [$F(T_{ref}=394 \text{ K}) = 147\text{s}$, $z=10^\circ\text{C}$]. The destruction of this organism and its toxin are of great public health significance in the processing of low acid foods, such as milk products.

In summary, the model was verified within the experimental range. However, the experimental film of water was not stable over film lengths long enough to approach the steam temperature. Therefore, further analysis is needed to determine actual temperature rise and bacterial destruction in a disintegrated film and attendant droplets. Although the experimental film was water, the model is general and is applicable to other low viscosity fluids such as fruit and vegetable juices, milk and milk products.

NOMENCLATURE

Roman Symbols

c_p	heat capacity, J/kg K
D	D value, s
F	F value, s
Fr	Froude number
g	gravitational constant, m/s ²
h	half thickness of film, m
k	thermal conductivity, J/m s K
k'	rate constant, s ⁻¹
L	film length, m
N	concentration or number of microorganisms, number/m ³
Pe	Peclet number
Q	mass flow rate, kg/m s
t	time, s
T	temperature, K
u	velocity in x-direction, m/s
We	Weber number
x	direction of flow, m
×	dimensionless direction of flow
y	direction perpendicular to flow, m
Y	dimensionless direction perpendicular to flow
z	direction in width of film, m
z	z value, K

Greek Symbols

δ	half thickness of the film, m
ρ	density, kg/m ³
σ	surface tension, N/m
θ	dimensionless temperature
ψ	dimensionless expression for velocity

Subscripts

o	initial
ref	reference
st	steam
T	temperature

REFERENCES

- BARRDAHL, R.A.G. 1988. Mass transfer in falling films: influence of finite-amplitude waves. *AIChE J.* **34**, 493–498.
- BROWN, D.R. 1961. A study of the behaviour of a thin sheet of moving liquid. *J. Fluid Mechanics.* **10**, 297–305.
- DOMBROWSKI, N. and JOHNS, W.R. 1963. The aerodynamic instability and disintegration of viscous liquid jets. *Chem. Eng. Sci.* **18**, 203–214.
- LIN, S.P. 1981. Stability of a viscous liquid curtain. *J. Fluid Mechanics.* **104**, 111–118.
- LIN, S.P. and ROBERTS, G. 1981. Waves in a viscous liquid curtain. *J. Fluid Mechanics.* **112**, 443–458.
- MCCARTHY, K.L. 1985. Sterilization of fluid foods by the free falling film method. Master's thesis, Department of Food Science and Technology, University of California, Davis.
- MCCARTHY, K.L. 1987. Steam infusion sterilization of a free falling film. Dissertation, Department of Agricultural Engineering, University of California, Davis.
- MURTY, N.S. and SASTRI, V.M.K. 1973. Flow of laminar falling liquid sheets and jets. Conference on Fluid Mechanics and Fluid Power, 4th. A.9.1.-A.9.6.
- MURTY, N.S. and SASTRI, V.M.K. 1974. Condensation on a falling laminar liquid film. *Heat Transfer.* **3**, 231–235.
- MURTY, N.S. and SASTRI, V.M.K. 1976. Condensation on a falling laminar liquid sheet. *Canadian J. Chem. Eng.* **54**, 633–635.
- RAO, V.D. and SARMA, P.K. 1984. Condensation heat transfer on laminar falling films. *J. Heat Transfer.* **105**, 518–523.
- SCRIVEN, L.E. and PIGFORD, R.L. 1959. Fluid dynamics and diffusion calculations for laminar liquid jets. *AIChE J.* **5**, 397–402.

A GENERALIZED VISCOSITY MODEL FOR EXTRUSION OF PROTEIN DOUGHS¹

R.G. MORGAN²

Kraft, Inc., Glenview, IL 60025

J.F. STEFFE and R.Y. OFOLI

*Department of Agricultural Engineering
and
Department of Food Science and Human Nutrition
Michigan State University
East Lansing, MI 48824-1323*

Accepted for Publication October 10, 1988

ABSTRACT

A theoretical model to predict the apparent viscosity of protein doughs during thermal processing involving heat induced denaturation is presented. The model allows viscosity prediction based on the effects of temperature-time history, strain history, temperature, shear rate and moisture content. Data from several sources have been considered in investigating the performance of the model. The approach facilitates an understanding of the mechanisms associated with protein texturization during extrusion.

INTRODUCTION

The need for a viscosity model which adequately describes process history effects on protein dough viscosities during extrusion is apparent. Such information is essential to accurate modeling and control of extrusion processes. Also, fundamental knowledge of effects of temperature-time history and strain history on dough viscosities should enhance the understanding of reaction kinetics involved in extrusion texturization. Viscosity models can also be useful in studying and predicting effects of process conditions on product quality.

¹Michigan Agricultural Experiment Station, Journal Article Number 1125

²Direct correspondence to Dr. Ron G. Morgan, Kraft, Inc., 801 Waukegan Road, Glenview, IL 60025 Telephone: (312)998-7440

Several researchers have attempted to model effects of moisture, temperature and shear rate on viscosity of corn flour and soy flour doughs. Jao *et al.* (1978) developed an empirical model for predicting effects of moisture, temperature and shear rate on apparent viscosity of soy dough during extrusion in a Brabender laboratory extruder. Their model was developed through multiple regression analysis. No attempt was made to estimate effects of temperature-time history. Cervone and Harper (1978) developed a four parameter model for correlating viscosity of extruded pregelatinized corn flour with moisture, temperature, and shear rate. Again, temperature-time history effects were not considered.

Remsen and Clark (1978) developed a model for predicting viscosity of cooking soy flour dough as a function of shear rate and temperature-time history by combining a temperature-shear model of soy flour dough (35% moisture) with a temperature-time history model of soy flour suspensions (70–75% moisture). They did not conduct tests on cooking doughs for determining temperature-time interaction, but assumed that relative increases in viscosity due to cooking were the same for concentrated flour suspensions as for doughs. Their model included a thermosetting relationship developed by Roller (1975) for curing of epoxy resins. As a result, the model exponentially approaches infinity for large temperature-time histories in contrast to experimental data (Morgan 1979) revealing that protein dough viscosities approach some finite maximum value for temperature-time histories and shear rates typically encountered in extrusion.

Most models are empirical and limited to observed experimental ranges. Bhat-tacharya and Hanna (1986) modeled effects of moisture and shear rate on viscosity of blends of corn gluten meal and soy protein concentrate. However, no attempt was made to account for thermal history. Very limited research has been conducted to model combined effects of temperature-time history on viscosity of protein doughs during extrusion. Morgan (1979) suggested that an integral temperature-time history is a primary factor on reaction kinetics of protein texturization. Janssen (1985) also recommends use of an integral temperature-time history term for modeling viscosity of extruded doughs. Luxenburg *et al.* (1985) concluded that both thermal and shear histories should be considered in modeling the extrusion process.

The objective of this study is to develop a practical model for predicting effects of viscometric shear rate, temperature, moisture content and temperature-time history on apparent viscosity of defatted soy flour dough undergoing heat induced protein denaturation. The model is an a priori development using reasonable analogies from polymerization kinetics and polymer rheology to predict changes in viscosities. The analogies are not necessarily meant to represent physicochemical reactions, but are aimed at predicting the outcome of these mechanisms as indicated by viscosity changes.

There are several problems encountered when attempting to draw analogies between plastic polymers and protein reactions. Polymers undergo various reversible melting and irreversible polymerization reactions during thermoplastic extrusion. However, proteins undergo irreversible complex denaturation kinetics with network entanglement or interlocking and possible crossbinding. In protein denaturation, several higher order reactions may occur simultaneously or in cascade.

Soy protein denaturation is more complex than a first order reaction. However, a simple reaction analogy is believed to be appropriate for estimating the average overall viscosity effects due to heat denaturation, temperature and shear of protein doughs over a finite range of conditions. The following development draws upon analogies between denaturation losses of macromolecular tertiary structure and the pseudo first order polymerization model. It assumes that increases in viscosity due to the unfolding and complexing of protein molecules or bodies are similar to the increases brought about by polymer molecular weight growth during a standard polymerization process.

MODEL DEVELOPMENT

The model is based on the combined theories of how temperature and shear rate affect viscosity of non-Newtonian fluids and “protein polymerization” reaction kinetics. A theoretical approach to rheological modeling of protein doughs provides for better understanding of mechanisms responsible for protein texturization during extrusion. Also, models developed from theory or theoretical analogies usually yield more practical limits and significantly reduce the costs of experimentation. The following mathematical development is based on laminar viscometric flow of incompressible, isotropic and homogeneous fluids.

Shear Rate Effects

Materials such as polymer solutions, protein slurries and doughs are typically described as non-Newtonian fluids. The most widely used non-Newtonian model is the Ostwald-de Waele (power law) model:

$$\tau = m \dot{\gamma}^{n-1} \quad [1]$$

Some investigators have modeled apparent viscosity of corn, oat and some protein doughs during extrusion processes assuming them to be shear-thinning (Harmann and Harper 1973 and 1974; Cervone and Harper 1978; Remsen and Clark 1978) and reported values of n from 0.25 to 0.51.

Although popular, there are two serious drawbacks of the power law model for predicting behavior of protein doughs: (1) It predicts unlimited decreasing apparent viscosity with increasing shear rate. (2) For a given value of n it predicts zero or infinite values of zero-shear viscosity. Another problem arising from applying Eq. [1] to protein doughs is that these materials usually exhibit a yield stress which is not accounted for by the power law model.

Luxenburg *et al.* (1985) observed significant yield stresses for 50% moisture defatted soy flour heated at 25, 50, 75, 85, 100 and 110 °C. They compared statistical fits of the power law and modified Bingham (Herschel-Bulkley) models and reported temperature dependent problems with the latter model: inconsistency in n and a cyclical dependence of m . No attempt was made to separate temperature-time history from temperature effects. It should be noted that the Herschel-Bulkley model approaches zero viscosity at high shear rates and may have limitations for high-shear extrusion modeling.

A simple relation known as the "Casson equation" (Casson 1959) was investigated by Morgan (1979) to model the apparent viscosity of protein doughs:

$$\sqrt{\tau} = \sqrt{\tau_o} + \sqrt{\mu_{\infty}\dot{\gamma}} \quad [2]$$

and

$$\eta(\dot{\gamma}) = \left[\sqrt{\frac{\tau_o}{\dot{\gamma}}} + \sqrt{\mu_{\infty}} \right]^2 \quad [3]$$

The power law model usually fits observed data with more accuracy than the Casson model for a limited shear rate range. In some cases, the Casson model fits observed data with an acceptable degree of accuracy and yields more reliable predictions at high and low shear rates. Darby (1976) has summarized three and four parameter models (Ellis, Meter, Cross, Reiner-Philippoff, etc.) which meet some of the criteria discussed above and are commonly used for modeling polymer solutions and suspensions.

A simple rheological model for protein doughs which provides for a finite yield stress, high shear limiting viscosity, and a variable shear thinning index is needed. Heinz (1959) proposed the following model, originally for chocolate, which fulfills the necessary requirements.

$$\eta(\dot{\gamma}) = \left[\left(\frac{\tau_o}{\dot{\gamma}} \right)^n + \mu_{\infty}^n \right]^{\frac{1}{n}} \quad [4]$$

This equation will be referred to in this study as the Heinz-Casson model (some may refer to it as a generalized Casson model). Equation [4] was chosen for predicting steady shear effects in this study because of its ability to meet the above criteria while maintaining some mathematical simplicity.

Temperature Effects

It is widely accepted that the influence of temperature on the viscosity of a Newtonian fluid can be represented by the relationship developed from the Eyring kinetic theory (Glasstone *et al.* 1941):

$$\mu = \mu_1 e^{\left(\frac{\Delta E_v}{RT}\right)} \quad [5]$$

Bird *et al.* (1960) define ΔE_v as the molar “free energy of activation” in a stationary fluid. It is related to the amount of molecular energy required for a molecule to escape its present surrounding (cage) and move into an adjoining molecular site (hole) while exposed to a defined velocity gradient.

Metzner (1959) proposed that Eq. [5] can be used for estimating temperature effects on the consistency coefficient of a shear-thinning fluid. He also assumed the flow index to be relatively independent of temperature. If one assumes that the Heinz-Casson coefficients τ_0 and μ_∞ are related to temperature by expressions similar to Eq. [5], and that n is independent of temperature, then Eq. [4] can be revised to account for temperature and shear rate effects:

$$\eta(\dot{\gamma}, T) = e^{\frac{\Delta E_v}{R}(T^{-1} - T_r^{-1})} \left[\left(\frac{\tau_r}{\dot{\gamma}} \right)^n + \mu_r^n \right]^{\frac{1}{n}} \quad [6]$$

where $\tau_T = \tau_0$ and $\mu_T = \mu_\infty$ at some reference temperature T_r . Harper (1981) reported that several authors have used the power law model for food doughs, in which n was assumed to be independent of temperature over specific temperature ranges.

Moisture Effects

Cervone and Harper (1978) used a semi-empirical logarithmic mixing rule to describe effects of moisture content on viscosity of corn flour dough. Harper *et al.* (1971) suggested a logarithmic relationship of moisture to dough viscosity. From that work, an equation for estimating effects of moisture on apparent viscosity of protein doughs for a steady shear rate and temperature can be presented (note that b is a negative coefficient):

$$\eta(MC) = \eta_{MC} e^{b(MC)} \quad [7]$$

Eq. [7] may be combined with Eq. [6] to give a relationship which combines steady shear rate, temperature and moisture content effects on apparent viscosity:

$$\eta(\dot{\gamma}, T, MC) = e^{\frac{\Delta E_v}{R}(T^{-1} - T_r^{-1}) + b(MC - MC_r)} \left[\left(\frac{\tau_r}{\dot{\gamma}} \right)^n + \mu_r^n \right]^{\frac{1}{n}} \quad [8]$$

where τ_r and μ_r are measured at reference temperature T_r and reference moisture content MC_r . Also, the previous development assumes that τ_0 and μ_∞ are similarly related to temperature by ΔE_v and to moisture content by b .

Temperature-Time History

Up to this point no attempt has been made to account for temperature-time history effects on apparent viscosity of protein doughs. As dough temperature exceeds its denaturation threshold temperature (T_d), protein molecules undergo various denaturation reactions affecting their size, shape and molecular weight. Since viscosity is related to all three, it is logical to assume that molecular changes caused by denaturation will significantly affect viscosity.

One hypothesis is that rheological and kinetic theory presently used in studying plastic polymers might be used as a starting point for modeling protein doughs in extrusion processes. Considerable theory has been developed for predicting polymerization phenomena of plastics and similar materials. Mathematical relationships have been developed using molecular and physical entanglement theories to predict rheological properties of polymers (Ferry 1970). Shah and Darby (1976) used molecular weight data to successfully predict apparent viscosity of polyethylene melts with weight average molecular weights ranging from 57,700 to 139,000.

As already discussed, several problems are encountered when analogies are drawn between reactions of plastic polymers and proteins in extrusion, because both the mechanisms and the order of reactions are different. Generally, first or second order reactions are assumed with reactive polymer and monomer species. However, in protein denaturation, several higher order reactions may occur simultaneously or in cascade. Huang (1983) concluded that disappearance of free amino groups of soy doughs could be predicted by a combination of first order and second order reactions. The rate and extent of these reactions will depend on temperature and temperature-time history, respectively.

The fact that protein doughs typically used in extrusion processing also contain mixtures of food ingredients other than protein must be considered. For example, protein and carbohydrates make up 90% (dry weight basis) of defatted soy flour. Soy carbohydrates contain no starch and consist primarily of the disaccharide sucrose, the trisaccharide raffinose and the tetrasaccharide stachyose (Smith and Circle 1972). Molecular weights of these polysaccharides are relatively small compared to proteins. As long as starch or oils are not present

with proteins, it is assumed that protein denaturation is the dominant reaction contributing to viscosity increases during the extrusion process. Huang (1983) concluded that carbohydrate concentrations of defatted soy flour, concentrate and isolate did not strongly affect the disappearance of free amino groups of extruded soy doughs.

A pseudo first-order kinetic model is used in this study to model temperature-time history effects of protein denaturation on apparent viscosity. Harper *et al.* (1978) successfully applied this approach to heat setting of Bovine plasma protein suspensions. Pseudo first-order polymerization assumes that concentration of one reactive species, the reactive polymer species, will remain constant and predicts disappearance of the monomer species.

Soy protein denaturation is more complex than a first-order reaction. However, a simple reaction can be used to approximate the "average-overall-viscosity" effect due to denaturation of the major protein fractions. The following development draws upon the analogy between kinetic losses of macromolecular tertiary structure and pseudo first order polymerization. It assumes that increase in viscosity due to the "unfolding" of protein macromolecules is similar to the viscosity increase brought about by increased polymer molecular weight during a polymerization process.

The pseudo first-order reaction is described by

$$M_c(t) = M_c^o e^{-k_1 t} \quad [9]$$

where $M_c(t)$ is concentration of the monomer at time t , M_c^o is the initial monomer concentration, and k_1 is a first order reaction rate constant. The molecular weight of a polymer can be approximated by (Williams 1971)

$$MW_p = MW_m DP \quad [10]$$

where MW_p is the polymer molecular weight, MW_m is the monomer molecular weight, and DP the degree of polymerization. Williams (1971) approximated DP as

$$DP = \frac{M_c^o - M_c}{P_c} \quad [11]$$

where P_c is the reactive polymer species concentration.

Ferry (1970) reports a power law relationship for correlating the zero shear rate limiting Newtonian viscosity (η_o) of polymers with their molecular weight:

$$\eta_o = k_2 (MW_p)^\alpha \quad [12]$$

where k_2 is a viscosity coefficient and α a dimensionless constant.

Theoretically, α is 1.0 and 3.5 for low and high molecular weight polymers, respectively. Shah and Darby (1976) report that observed values of α found in the literature range from 3.4–8.0 for high molecular weight polymers. Eq. [12] cannot be used directly for modeling effects of molecular weight on apparent viscosity without knowing the relationship between η_0 and η . However, if biological doughs have a yield stress, then η_0 is not a relevant parameter at low shear rates.

Collins and Bauer (1965) present a relationship describing the effects of molecular weight (MW_p) and shear rate on the apparent viscosity of high molecular weight polymers. They used data of Ballman and Simon (1964) for polystyrene as supporting evidence of their theory. Collins and Bauer (1965) indicate that onset of non-Newtonian behavior is highly dependent on molecular weight. The molecular weight corresponding to onset increases as shear rate decreases. After onset of non-Newtonian flow, η versus MW_p at constant $\dot{\gamma}$, appears to approach a power-law relationship at some higher molecular weight:

$$\eta = k_2^1 (MW_p)^{\alpha(\dot{\gamma})} \quad [13]$$

where k_2^1 is a viscosity coefficient similar to k_2 and is related to $\dot{\gamma}$, T and MC according to Eq. [8]. The exponent α is a function of $\dot{\gamma}$. This relationship is similar to Eq. [12] with α being dependent on $\dot{\gamma}$. Theoretically, α is 3.4 for very low shear rates and approaches zero as $\dot{\gamma}$ approaches infinity. Analysis of Ballman and Simon's (1964) data reveals that for a given MW_p , α is approximately related to $\dot{\gamma}$ by a power law equation of the form,

$$\alpha = \alpha_0 \dot{\gamma}^a \quad [14]$$

for $\dot{\gamma} > 1$. The exponent a is negative, causing α to approach zero for large shear rates, which is demonstrated by the Ballman and Simon (1964) data. The parameter α_0 relates to the onset of non-Newtonian behavior which for polymers is shown to be highly dependent on molecular weight. The parameter α_0 relates to an "effective molecular weight" of the denatured proteins, while a is a relative measure of the shape and tendency of entanglement of the unfolding proteins during heating and shearing.

To incorporate the "psuedo-molecular-weight-effects" it is assumed that viscosity of a denaturing protein dough can be described by

$$\eta = \eta_{ud} + \Delta\eta_{MW} \quad [15]$$

where η_{ud} represents the undenatured viscosity described by Eq. [8] and $\Delta\eta_{MW}$ represents the increase in viscosity due to "unfolding" of "protein macromolecules" and can be represented by a relationship similar to Eq. [13].

$$\Delta\eta_{MW} = \beta (MW_p)^{\alpha(\dot{\gamma})} \quad [16]$$

It is assumed that β is a denaturation viscosity material coefficient, similar to k_2^1 , which depends upon η , T and MC similar to Eq. [8], hence

$$\beta = \beta_r e^{\frac{\Delta E_d}{R}(T^{-1} - T_r^{-1}) + b(MC - MC_r)} \left[\left(\frac{\tau_r}{\dot{\gamma}} \right)^n + \mu_r^n \right]^{\frac{1}{n}} \quad [17]$$

where β_r is a material constant. Note that $\Delta\eta_{MW}$ is zero if temperature has never reached or exceeded the denaturation threshold, T_d .

Equations [9], [10], and [11] are combined with Eq. [16] yielding $\Delta\eta_{MW}$ as a function of reaction time (t), for constant temperature T:

$$\Delta\eta_{MW} = \beta \left(\frac{MW_m M_c^o}{P_c} \right)^{\alpha(\dot{\gamma})} (1 - e^{-k_1 t})^{\alpha(\dot{\gamma})} \quad [18]$$

Equation [18] describes the relative increase in protein dough viscosity due to heat-induced denaturation. This increase is a function of time for all temperatures (T) greater than the threshold temperature (T_d).

The pseudo first-order reaction (Eq. 9) used in developing Eq. [18] assumes that temperature is constant and greater than the reaction threshold temperature. The coefficient k_1 is defined as the polymerization rate constant. Absolute reaction theory (Eyring and Stearn 1939) implies that k_1 is related to temperature by

$$k_1 = k_\infty e^{\left(\frac{-\Delta E_d}{RT} \right)} \quad [19]$$

where k_∞ is a specific reaction constant and ΔE_d is the activation energy of protein denaturation. According to Eyring and Stearn (1939), k_∞ is related to absolute temperature by

$$k_\infty = \left(\frac{k_t k_b}{h} \right) T \quad [20]$$

where k_t is a transmission coefficient (usually taken as unity), k_b is Boltzman's constant and h is Planck's constant.

Application of Eq. [19] and [20] to Eq. [18] requires that temperature remain constant with time. However, in an extrusion process, the dough temperature will increase from its initial ambient temperature to a maximum and, possibly,

be reduced before exiting the die. Therefore, each process will result in a distinct temperature-time history creating a need for a method to incorporate variable temperature-time histories into Eq. [18]. To meet this need, an integral temperature-time history function, ψ , is defined:

$$\psi = \int_0^t T(t) e^{\left(\frac{-\Delta E_d}{RT(t)}\right)} dt \quad [21]$$

with $T(t) \geq T_d$ for all $t > 0$ and ψ is defined as zero for all time during which $T \leq T_d$. ψ is related to Eq. [14] through the following expression:

$$k_1 t = k_a \psi \quad [22]$$

where

$$k_a = \frac{k_i k_b}{h} \quad [23]$$

and represents a reaction transmission coefficient for the material protein source. Equations [15], [17], [18], [21], and [22] are combined with Eq. [8] to give a combined viscosity for the undenatured and denaturing cases in terms of $\dot{\gamma}$, T , MC and T - t history:

$$\eta(\dot{\gamma}, T, MC, \psi) = e^{\frac{\Delta E_v}{R}(T^{-1} - T_r^{-1}) + b(MC - MC_r)} \left[\left(\frac{\tau_r}{\dot{\gamma}} \right)^n + \mu_r^n \right]^{\frac{1}{n}} \left[1 + \beta_r \left(\frac{MW_m M_c^o}{P_c} \right)^{\alpha(\dot{\gamma})} (1 - e^{-k_a \psi})^{\alpha(\dot{\gamma})} \right] \quad [24]$$

It is not practical to attempt to quantify MW_m , M_c^o and P_c in Eq. [24] for food proteins. However, the ratio M_c^o/P_c is analogous to an "effective concentration" of reacting species, in this case the undenatured protein concentration on a dry weight basis. For most protein doughs, the moisture content is low enough so unfolding phenomena are directly affected by the amount of available water. That is, water content is a limiting factor in the relative viscosity effects of protein denaturation for a given thermal history. Therefore, it is

assumed that the MW_m term can be used as a relative measure of the positive effects of water on the extent of the hydration and subsequent unfolding of proteins when heated. The following two models are proposed for relating the effects of protein concentration and moisture on MW_m , M_c^o , P_c for a given range of MC.

$$MW_m = A_1 MC^\epsilon \quad [25]$$

$$\frac{M_c^o}{P_c} = A_2 C_p \quad [26]$$

where A_1 , A_2 and ϵ are material constants which depend on protein source and the initial undenatured state. Note that MW_m is not the true molecular weight of undenatured protein, but rather a pseudo MW relative to that of the denatured state, MW_p . Equations [14], [25], and [26] were combined with Eq. [24] to obtain the final viscosity model:

$$\eta(\dot{\gamma}, T, MC, \psi) = e^{\frac{\Delta E_v}{R}(T^{-1} - T_r^{-1}) + b(MC - MC_r)} \left[\left(\frac{\tau_r}{\dot{\gamma}} \right)^n + \mu_r^n \right]^{\frac{1}{n}} \left[1 + \beta_r [A_3 (MC)^\epsilon C_p]^{\alpha_o \dot{\gamma}^a} \right]. \quad [27]$$

$$\left[(1 - e^{-k_a \psi})^{\alpha_o \dot{\gamma}^a} \right]$$

where

$$A_3 = A_1 A_2 \quad [28]$$

Shear History

Relatively little is known about the effects of extrusion shear-strain history on protein dough viscosity. Bruin *et al.* (1978) suggest that the weighted-average shear-strain history concept should be applied when modeling extrusion of biological materials. However, the authors were unable to locate any published literature where an attempt was made to quantify shear-history effects on viscosity of extruded food doughs. Huang (1983) correlated screw speed with the disappearance of free amino groups. He used various scenarios of reaction models to attempt to model the disappearance of free amino groups as a function of screw-speed, with residence time being inversely related to screw speed. Huang (1983) made no attempt to quantify strain-history or thermal history.

One would expect that effects of strain-history (Φ) on apparent viscosity will be a decreasing function approaching an equilibrium asymptote as $\Phi \rightarrow \infty$. Therefore, the following expression is proposed for approximating strain-history effects of η at given T , MC , $\dot{\gamma}$ and ψ :

$$\eta = \eta_o^1 - (\eta_o^1 - \eta_\infty)(1 - e^{-d\Phi}) \quad [29]$$

where η_o^1 is the value of η at $\Phi = 0$ and is given by Eq. [27]. η_∞ is the asymptote of η as $\Phi \rightarrow \infty$, and d is a first order rate constant. The parameter d is most likely dependent upon the average $\dot{\gamma}$ experienced during the accumulation of Φ . Little experimental data exist from which to quantify η_∞ and the effects of $\dot{\gamma}$ on d . The problem arises from the difficulty of obtaining $\dot{\gamma}$ versus time distribution data within an extruder in order to quantify Φ .

At this point, the authors suggest that Eq. [29] serve as an effective starting point for incorporating strain-history effects into the generalized model of Eq. [27]. Rearranging Eq. [29] yields

$$\frac{\eta}{\eta_o^1} = 1 - \frac{\eta_o^1 - \eta_\infty}{\eta_o^1}(1 - e^{-d\Phi}) \quad [30]$$

$$\frac{\eta}{\eta_o^1} = 1 - \beta_o(1 - e^{-d\Phi}) \quad [31]$$

where

$$\beta_o = \frac{(\eta_o^1 - \eta_\infty)}{\eta_o^1} \quad [32]$$

the relative amount of viscosity reduction due to strain-history effects.

Generalized Model

Combining Eq. [27] and [31] yields the general model form of

$$\eta(\dot{\gamma}, T, MC, \psi, \Phi) = e^{\frac{\Delta E_v}{R}(T^{-1} - T_r^{-1}) + b(MC - MC_r)} \left[\left(\frac{\tau_r}{\dot{\gamma}} \right)^n + \mu_r^n \right]^{\frac{1}{n}} \left[1 + \beta_r [A_3(MC)^{\epsilon} C_p]^{\alpha_o \dot{\gamma}^a} \right] \left[(1 - e^{-d\psi})^{\alpha_o \dot{\gamma}^a} [1 - \beta_o(1 - e^{-d\Phi})] \right] \quad [33]$$

The description and physical meaning of the constants and coefficients in Eq. [33] are summarized in Table 1.

TABLE 1.
DESCRIPTION AND PHYSICAL SIGNIFICANCE OF CONSTANTS
AND COEFFICIENTS USED IN EQ. [33]

Parameter	Physical Meaning/Description
a	Power law coefficient relating shear-rate effects on the molecular weight of denatured protein
A_3	Dimensionless material constant related to the effective molecular weight of the protein
b	Exponent quantifying the lubricating effects of moisture on dough viscosity
C_p	Protein concentration, dry weight basis
d	Rate constant quantifying effects of thixotropy
ΔE_v	Viscous activation energy of temperature effects
k_a	Protein denaturation reaction constant
n	Heinz-Casson shear thinning index
α_0	Intercept coefficient relating the effect of denatured protein molecular structure on viscosity at low shear rates
β_0	The relative magnitude of maximum effects of thixotropy
β_T	Material constant related to the maximum viscosity increase due to protein gelation
ϵ	Exponent relating effects of moisture level to the extent of protein denaturation
μ_T	High shear limiting viscosity of the undenatured dough at the reference temperature
τ_T	Pseudo yield stress of the undenatured dough at the reference temperature

RESULTS AND DISCUSSION

Data from Morgan (1979), Luxenburg *et al.* (1985) and Huang (1983) were used to evaluate the proposed model for soy protein doughs made from defatted flour (55% protein, dry basis), concentrate mixture (76% protein) and isolate (95% protein). Morgan (1979) used a capillary rheometer to evaluate effects of

moisture, temperature, cook temperature-time history, and shear rate on the apparent viscosity of defatted soy flour dough. Luxenburg *et al.* (1985) conducted capillary rheometer studies to evaluate effects of temperature and shear rate on the apparent viscosity of defatted soy flour. Huang (1983) conducted extrusion cooking tests with a Haake Rheodrive model Mixer/Extruder, with a 0.75 in diameter, 28 L/D barrel. Huang (1983) investigated effects of moisture content, barrel zone temperature and screw speed on an apparent viscosity analogue and the disappearance of free amino groups for defatted soy flour, soy isolate and a mixture of the two yielding 76% protein (d.b.) as an effective concentrate. Huang (1983) did not correct die pressure drop versus flow rate data for entrance effects, hence the term "apparent viscosity analogue" (AVA). The AVA values were, consequently, significantly larger in magnitude than the true apparent viscosities. Therefore, the AVA data could only be used to verify effects of protein content and temperature-time history on relative changes in viscosity.

Table 2 contains a summary of the range of experimental variables for data obtained from each of the literature sources. Observed shear rate versus apparent viscosity data were extracted from the published sources along with corresponding moisture, protein, temperature, hold time, and average shear rate during the cook cycle.

Data from Morgan (1979) and Luxenburg *et al.* (1985) were used to evaluate model parameters of Eq. [33] using an iterative linear regression technique. Equation [33] was first analyzed for all data in which $\psi = 0$. Whenever the resulting form of Equation [33] could not be transformed to an explicit linear relationship, appropriate terms were grouped and the constraining variables initialized. Then standard least-squares linear regressions were performed in an iterative fashion until the optimum value was obtained for each constraining variable.

Model accuracy and effectiveness are depicted by a composite graph of observed data versus predicted values (Fig. 1). It is important to note the ability of the model to adequately predict viscosities from 1 to 1,000,000 for a wide range of process conditions. The accuracy of Eq. [33] is much higher when fit only to one data source. However, the objective of this work was to develop and prove a versatile model for a wide range of applications. Table 3 contains best fit values for each model parameter in the composite analysis of all three data sources.

Note that the data of Morgan (1979) and Luxenburg *et al.* (1985) plotted in Fig. 1 have a strain history (Φ) equal to zero. Huang (1983) conducted his study using a small lab extruder, hence significant strain histories were imparted. Operating conditions and extruder geometry data from Huang (1983) were used to estimate the range of Φ reported in Table 2. The model consistently over-predicted the data of Huang (1983), one possible reason being that strain history effects were not included. This emphasizes the need for future research aimed at

TABLE 2.
SUMMARY OF EXPERIMENTAL CONDITIONS FOR
VISCOSITY DATA USED IN THIS STUDY

Source	Ingredient Base	Experimental Device	Protein Content (% d.b.) Cp	Moisture Level (% w.b.) MC	Temperature (°C) T _i	Hold Time (min) Δt	Shear Rate (s ⁻¹) γ̇	Shear History φ (2)
Morgan (1979)	Defatted Soy Flour	Capillary Rheometer	55	29-39	24-150	0.5-2.5	1.6-1630	0
Luxemburg et al. 1985	Defatted Soy Flour	Capillary Rheometer	55	54	25-110	21 (1)	2-1300	0
Huang (1983)	Defatted Soy Flour Isolate	Haaker Mixer/Screw Extruder	56,76, 96	30	100-150	30-160	3-30	2000-5000

(1) The authors reported that the average length of an experimental run was approximately 30 min, with steady state measurements taken during the last 15 minutes. About 2-3 minutes are required to obtain mass average temperatures that are 99% of the barrel temperature, therefore, 20 minutes was used as a mean effective cook time within the C.R.

(2) $\phi = \Delta t \cdot \bar{\gamma}$; $\bar{\gamma}$ = average shear rate in extruder screw channel

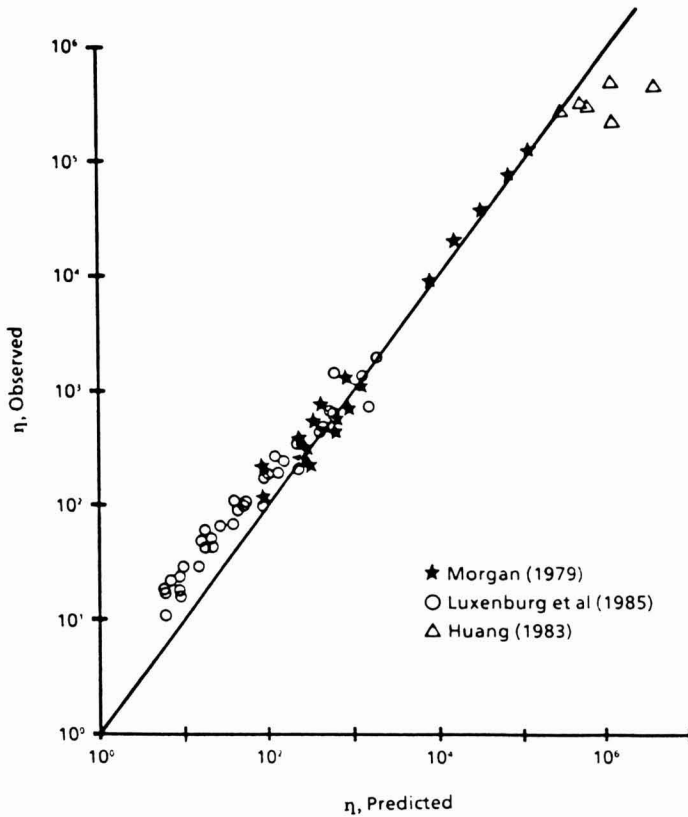


FIG. 1. APPARENT VISCOSITY PREDICTIONS USING EQ. [33] VERSUS EXPERIMENTAL OBSERVATIONS

quantifying the strain history effects in Eq. [33]. No attempt was made in this study to quantify the model parameters of Φ .

Viscosity data presented by Luxenburg *et al.* (1985) were used to demonstrate the usefulness of the modeling technique developed in this study. Actual viscosity versus shear rate data were extracted from Fig. 2 of Luxenburg *et al.* (1985) for all temperature treatments from 25 °C to 110 °C. The data were replotted and curve fitting techniques used to provide estimates of viscosity at various temperatures and heat treatments at the same shear rate. Equation [5] was used to adjust all data to a common reference temperature of 68 °C and Eq. [21] used to compute temperature-time histories.

At 25 °C and 50 °C, no significant protein denaturation occurs, making the temperature adjusted viscosities very similar (Fig. 2). As temperature exceeds

TABLE 3.
MODEL CONSTANTS AND COEFFICIENTS FOR EQ. [33]
WITH DEFATTED SOY FLOUR DOUGH

Parameter	Best Fit Value	Comments
a	-0.15	-0.30 for polystyrene (Collins & Bauer, 1965)
A ₃	12.3	No literature reference
b	-21	Normally ranges from -6 to -18
d	N.D.	Insufficient data to quantify
ΔE _v (Kcal/gmole)	6.8	Commonly reported as 4.0-8.0 for food doughs
k _a (K s) ⁻¹	13.9 × 10 ¹⁰	2.08 × 10 ¹⁰ for theoretical transmission coefficient of 1
n	0.30	Within ranges reported in literature (0.2-0.5)
α ₀	2.0	2.42 for polystyrene (Collins & Bauer 1965)
β ₀	N.D.	Insufficient data to quantify
β _r	1.16	No literature reference
μ _r (Pa s)	21.0*	No literature reference
τ _r (kPa)	32.8*	No literature reference

*Reference temperature = 68 °C

the 65–70 °C level, typically considered the denaturation threshold for soy protein, significant increases in viscosity occur (Fig. 2). The heat denaturation causes the protein to unfold and entangle or interlock, increasing apparent viscosity. The 100 °C and 110 °C treatments were both sufficient to fully denature the proteins (Fig. 2). This does not imply that the reactions at 100 °C are exactly the same as those at 110 °C. Rather, the model assumes, and these data suggest, that the net impact on viscosity for both treatments should be similar, given that treatment time is sufficient to achieve nearly complete reaction.

The net increase in viscosity due to protein denaturing is offset by an increase in shear rate. Increasing shear is believed to physically disrupt the interlocking effects causing a reduction in the overall increase in apparent viscosity (Fig. 2). Some authors (Luxenburg *et al.* 1985; Jao *et al.* 1978) have reported viscosity data and attempted to explain effects of various thermal histories without adjusting for the temperature effects of Glasstone *et al.* (1941). This has resulted in confusing and contradicting interpretations regarding the influences of heat denaturation on the viscosity of protein doughs. The information illustrated in Fig. 2 shows that the modeling technique presented in this work can be used to enhance the basic understanding of physical and chemical mechanisms involved in the cooking of protein doughs.

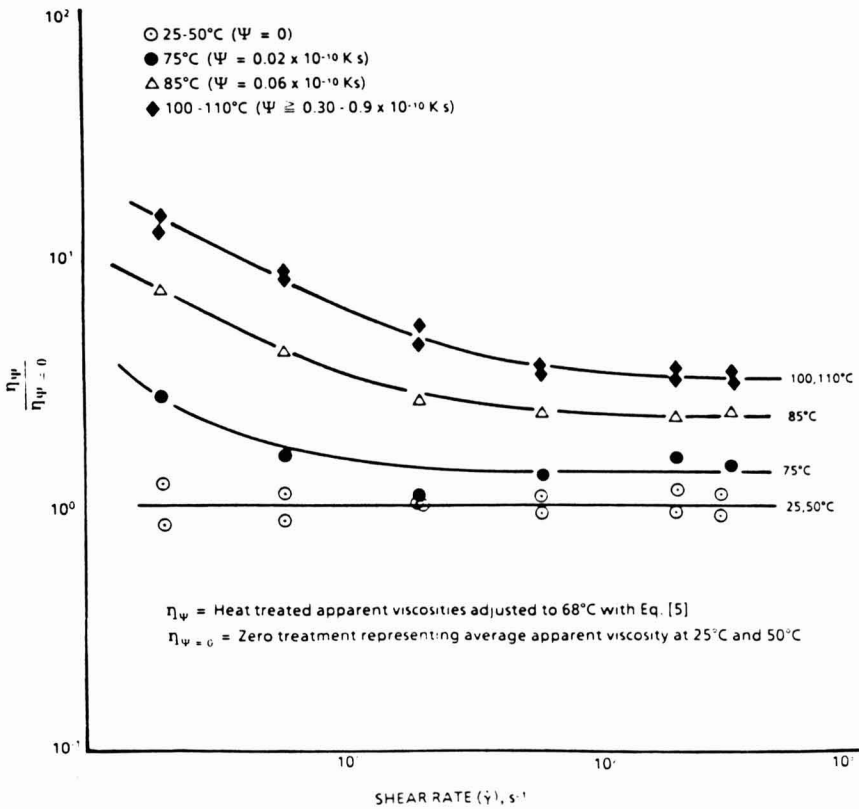


FIG. 2. APPLICATION OF THE MODEL TO LUXENBURG *ET AL.* (1985) DATA DEMONSTRATING THE EFFECTS OF HEAT TREATMENT AND SHEAR HISTORY ON VISCOSITY

The modeling approach presented in this work results in a consistent interpretation of the effects of various heat treatments on apparent viscosity for data (Fig. 3) taken from two independent sources: Luxenburg *et al.* (1985) and Morgan (1979). Once again, note the importance of separating the Glasstone temperature effects (Eq. [5]) before attempting to interpret heating effects. Even though there is some variability, it is clear that the trends in the Morgan 1979 data are very similar to those from Luxenburg *et al.* (1985) for a shear rate of 326 s^{-1} . Also, note the typical first-order reaction profile at each shear rate.

As previously noted in the development of Eq. [14], shear rate significantly influences molecular weight effects on viscosity (Ballman and Simon 1964). Polystyrene data were extracted from the work of Collins and Bauer (1965) and compared to soy protein dough data from Luxenburg *et al.* (1985) and Morgan

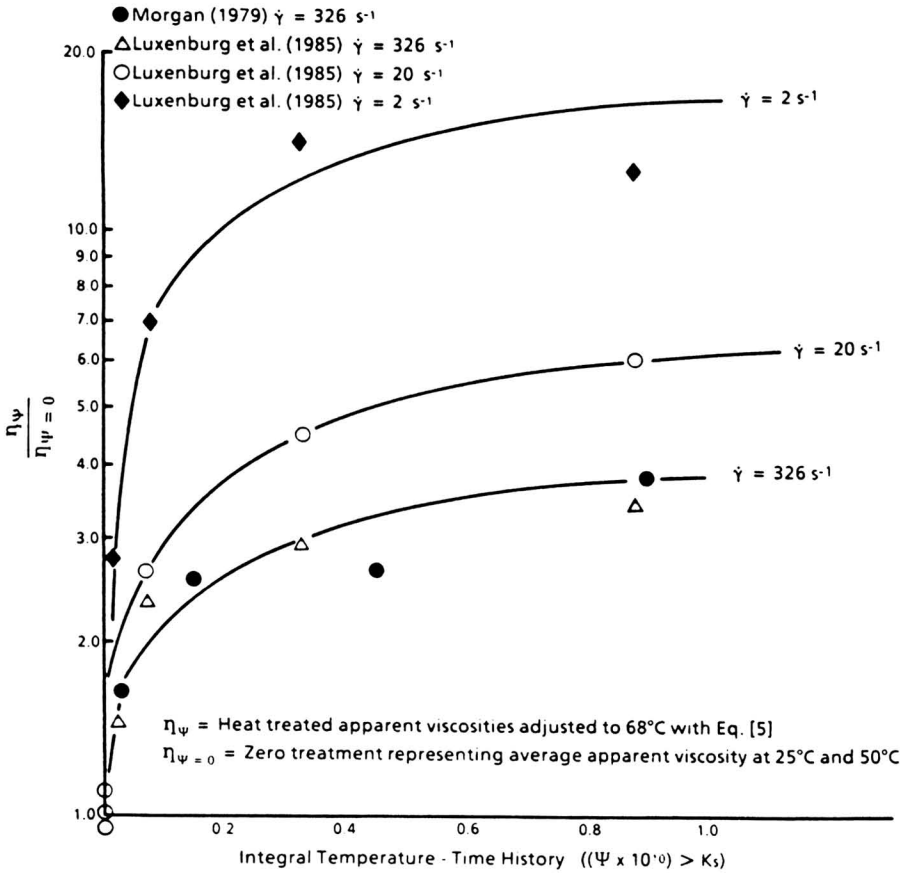
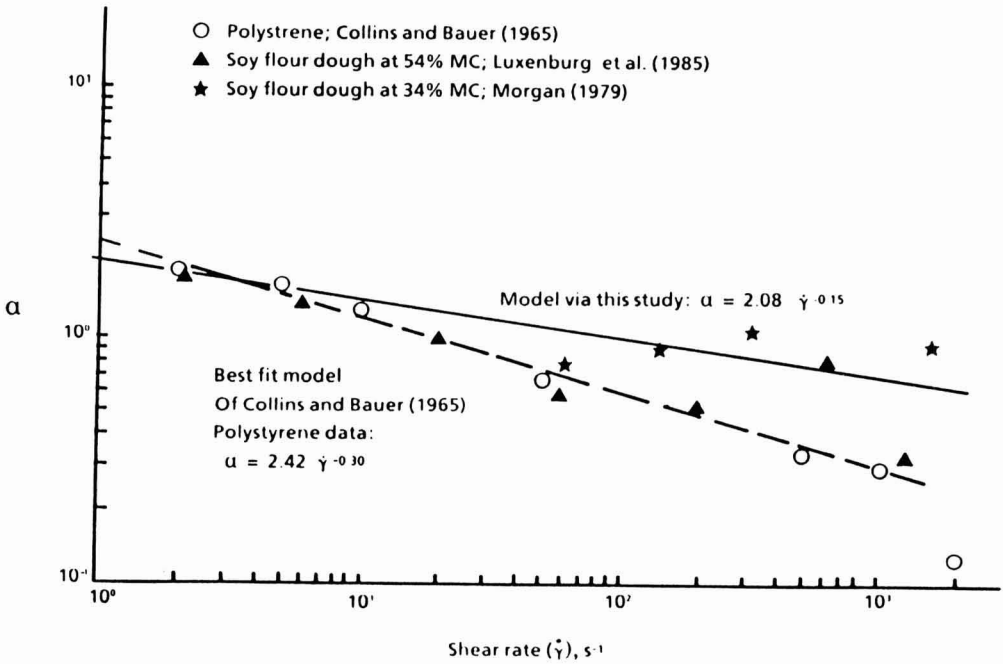


FIG. 3. EFFECT OF INTEGRAL TEMPERATURE-TIME HISTORY ON VISCOSITY AT VARIOUS SHEAR RATES

(1979) in predicting the effects of $\dot{\gamma}$ on α . Data from Luxenburg are close to those for polystyrene while data from Morgan (1979) are higher for shear rates exceeding 100 s^{-1} (Fig. 4). This may be due to the difference in moisture content between the Luxenburg data (MC = 54%) and Morgan data (MC = 34%). The difference does not necessarily mean the assumption underlying Eq. [14] are erroneous. Rather, sizable experimental error could have been induced by slip at the lower moisture content. Further research is needed to verify Eq. [14].

Another possible cause for the variation in data between literature sources is the fact that no attempts were made to correct for slip. In each of the three studies, different die materials and designs were used, thus causing significant variations in how slip may have affected the data.

FIG. 4. EFFECTS OF SHEAR RATE ON α

The approach presented in this study is not a literal, theoretical application of predicting physical or molecular mechanisms. Rather, it is a common-sense approach to modeling the complex nature of a commonly processed material in food extrusion. The value of this work is demonstrated by the fact that the model adequately predicts the viscous behavior of protein doughs over a broad range of process conditions for three independent studies. Subsequent publications will deal in further detail with specific performance of various portions and assumptions of the model. The purpose of this publication is to show that the general approach is valid in developing practical food rheology models.

SUMMARY AND CONCLUSIONS

A theoretical model has been presented for predicting effects of shear rate, temperature, moisture content and temperature-time history on the apparent viscosity of defatted soy flour dough undergoing heat-induced protein denaturation. Temperature effects were modeled using the popular Arrhenius relationship. The Heinz-Casson model was used to predict shear rate effects and provides a finite high-shear limiting viscosity, a variable shear thinning index, and a

finite yield stress. Temperature-time history effects were modeled by approximating protein denaturation effects as a pseudo first-order polymerization reaction. An integral temperature-time history function was used to incorporate effects of variable thermal histories.

The model was derived under the following simplifying assumptions:

- (1) Pseudo first-order protein denaturation reaction kinetics
- (2) Viscometric shear, and
- (3) Effects of composition, other than protein and moisture, are negligible.

Analysis of experimental data from Morgan (1979), Luxenburg (1985), and Huang (1983) indicate that the model adequately predicts effects of shear rate, temperature, moisture content and temperature-time history on apparent viscosity of defatted soy dough for a wide range of conditions. Several of the model parameters are in good agreement with those found in the literature. An important characteristic of the model is that it predicts finite values of viscosity for large values of shear rate, temperature and temperature-time history. For values outside the observed experimental range, general behavior of the model is realistic.

The general viscosity model developed in this study should prove useful in modeling flow rates and power requirements of screw extruders. Also, this model can add insight to the basic understanding of protein texturization phenomena. This type of modeling, which is based on fundamental sciences of polymer rheology and protein chemistry, offers a useful scientific tool for future research of plant protein dough and their reactions during processing.

Additional studies are needed for further defining strain history effects and for further validation of the proposed model. Research is also needed to incorporate viscoelastic properties and the effects of industrial processing additives on model parameters.

NOMENCLATURE*

b	dimensionless moisture coefficient
h	Planck's constant
k_b	Boltzman's constant
k_1	first-order reaction rate constant (1/t)
k_2	viscosity coefficient (Ft/L ²)
k_2^j	viscosity coefficient (Ft/L ²)
k_t	transmission coefficient
k_∞	specific reaction velocity constant (1/t)
m	Power law consistency coefficient (Ft/L ²)

n	Power law flow index, dimensionless
t	time (t)
DP	average degree of polymerization
ΔE_d	protein denaturation activation energy (FL/mole)
ΔE_v	activation energy of viscosity (FL/mole)
M_c	monomer concentration at time t
M_c°	initial monomer concentration
MC	moisture content, decimal wet basis
MW_m	monomer molecular weight
MW_p	polymer molecular weight
P_c	reactive polymer species concentration
R	universal gas constant (FL/mole-T)
T	absolute temperature (t)
T_d	threshold temperature for protein denaturation (T)
T_r	reference temperature (T)
α	dimensionless material function
α_0, a, β, Φ	dimensionless material constants
$\dot{\gamma}$	viscometric shear rate (L/T)
η	apparent viscosity (Ft/L ²)
η_{MC}	moisture viscosity coefficient (Ft/L ²)
η_{ud}	undenatured viscosity (Ft/L ²)
$\Delta\eta_{MW}$	increase in viscosity due to unfolding of protein macromolecules (Ft/L ²)
η_0	zero shear rate limiting Newtonian viscosity (Ft/L ²)
μ	Newtonian viscosity (Ft/L ²)
μ_∞	Heinz-Casson model high shear rate limiting viscosity (Ft/L ²)
μ_1	Newtonian viscosity at infinite temperature (Ft/L ²)
μ_r	Heinz-Casson high-shear limiting viscosity at reference temperature T_r
τ	viscometric shear stress (F/L ²)
τ_0	Heinz-Casson model yield stress (F/L ²)
τ_r	Heinz-Casson yield stress at some reference temperature T_r
ψ	Integral temperature-time history function (t T)

* The symbols, F, L, M, T, and t indicate dimensions of force, length, mass, temperature and time, respectively.

REFERENCES

- BALLMAN, R.L. and SIMON, R. 1964. J. Polymer Sci. A2: 3557. (Cited in Collins and Bauer (1965)).
- BIRD, R.B., STEWART, W.E. and LIGHTFOOT, E.N. 1960. *Transport Phenomena*. John Wiley & Sons, New York.
- BHATTACHARYA, M. and HANNA, M.A. 1986. Viscosity modeling of dough in extrusion. J. Food Tech. 21, 167-174.
- BRUIN, S., VAN ZUILICHEM, D.J. and STOLP, W. 1978. A review of fundamental and engineering aspects of extrusion of biphymers in a single-screw extruder. J. Food Process Eng. 2, 1-37.
- CASSON, N. 1959. A flow equation for pigment-oil suspensions of the printing ink type. Ch. 5, In *Rheology of Disperse Systems*, (C.C. Mill, ed.), Pergamon Press.
- CERVONE, N.W. and HARPER, J.M. 1978. Viscosity of an intermediate moisture dough. J. Food Proc. Eng. 2, 83-95.
- COLLINS, E.A. and BAUER, W.H., 1965. Analysis of flow properties in relation to molecular parameters for polymer melts. Trans. Soc. Rheol. 9(2), 1-16.
- DARBY, R. 1976. *Viscoelastic Fluids, an Introduction to Their Properties and Behavior*. Marcel Dekker, New York.
- EYRING, H. and STEARN, A.E. 1939. The application of the theory of absolute reaction rates to proteins. Chemical Reviews, 24, 253-270.
- FERRY, J.D. 1970. *Viscoelastic Properties of Polymers*, 2nd ed. John Wiley & Sons, New York.
- GLASSTONE, S., LAIDLER, K.J. and EYRING, H. 1941. *Theory of Rate Processes*. McGraw-Hill, New York.
- HARMANN, D.V. and HARPER, J.M. 1973. Effect of extruder geometry on torque and flow. Transactions of the ASAE, 16, 1175-1176.
- HARMANN, D.V. and HARPER, J.M. 1974. Modeling a forming foods extruder. J. Food Sci. 39, 1100-1101.
- HARPER, J.M. 1981. *Extrusion of Foods*, Vol. 1, CRC Press, Boca Raton, FL.
- HARPER, J.M., RHODES, T.P. and WANNINGER, JR., L.A. 1971. Viscosity model for cooked cereal doughs. Amer. Inst. Chem. Engl. Symp. Serv. No. 108.
- HARPER, J.M., SUTER, D.A., DILL, C.W. and JONES, E.R. 1978. Effects of heat treatment and protein concentration on the rheology of bovine plasma protein suspensions. J. Food Sci. 43, 1204-1209.
- HEINZ, W. 1959. Quoted in Fincke, A. 1961. Beitrage zur Losung rheologischer Probleme in der Schokoladentechnologie, Dissertation, TH Karlsruhe.

- HUANG, B. 1983. Protein reactions in texturizing extruders. Ph.D. dissertation, Univ. of Massachusetts. Univ. Microfilm International, Ann Arbor, MI.
- JANSSEN, L.P.B.M. 1985. Models for cooking extrusion. Fourth International Congress on Engineering and Food. Edmonton, Alberta, Canada. July 7-10.
- JAO, Y.C., CHEN, A.H., LEWANDOWSKI, D. and IRWIN, W.E. 1978. Engineering analysis of soy dough rheology in extrusion. *J. Food Proc. Eng.* 2, 97-112.
- LUXENBURG, L.A., BAIRD, D.G. and JOSEPH, E.G. 1985. Background studies in the modeling of extrusion cooking processes for soy flour doughs. *Biotechnology Progress*, 1(1), 33-38.
- METZNER, A.B. 1959. Flow behavior of thermoplastics. In *Processing of Thermoplastic Materials*. (E.C. Bernhardt, ed.) Van Nostrand Reinhold Co., New York.
- MORGAN, R.G. 1979. Modeling the effects of temperature-time history, temperature, shear rate and moisture on viscosity of defatted soy flour dough. Ph.D. Dissertation, Agricultural Engineering, Texas A&M University, College Station.
- REMSEN, C.H. and CLARK, J.P. 1978. A viscosity model for a cooking dough. *J. Food Proc. Eng.* 2, 39-64.
- ROLLER, M.B. 1975. Characterization of the time-temperature-viscosity behavior of curing B-staged epoxy resins. *Pol. Eng. Sci.* 15(6), 406-414.
- SHAH, B.H. and DARBY, R. 1976. Prediction of polyethylene melt rheological properties from molecular weight distribution data obtained in complete citation by gel permeation chromatography. *Poly. Eng. Sci.* 16(8), 579-584.
- SMITH, A.K. and CIRCLE, S.J. 1972. Chemical composition of the seed. In *Soybeans: Chemistry and Technology*, (A.K. Smith and S.J. Circle, eds.) pp. 81-82, Van Nostrand Reinhold/AVI, New York.
- WILLIAMS, D.J. 1971. *Polymer Science in Engineering*. Prentice-Hall, Englewood Cliffs, New Jersey.

F N P PUBLICATIONS IN FOOD SCIENCE AND NUTRITION

Journals

JOURNAL OF MUSCLE FOODS, N.G. Marriott and G.J. Flick
JOURNAL OF SENSORY STUDIES, M.C. Gacula, Jr.
JOURNAL OF FOOD SERVICE SYSTEMS, O.P. Snyder, Jr.
JOURNAL OF FOOD BIOCHEMISTRY, J.R. Whitaker, N.F. Haard and
H. Swaisgood
JOURNAL OF FOOD PROCESS ENGINEERING, D.R. Heldman and R.P. Singh
JOURNAL OF FOOD PROCESSING AND PRESERVATION, D.B. Lund
JOURNAL OF FOOD QUALITY, R.L. Shewfelt
JOURNAL OF FOOD SAFETY, J.D. Rosen and T.J. Montville
JOURNAL OF TEXTURE STUDIES, M.C. Bourne and P. Sherman

Books

CONTROLLED/MODIFIED ATMOSPHERE/VACUUM PACKAGING OF
FOODS, A.L. Brody
NUTRITIONAL STATUS ASSESSMENT OF THE INDIVIDUAL, G.E. Livingston
QUALITY ASSURANCE OF FOODS, J.E. Stauffer
THE SCIENCE OF MEAT AND MEAT PRODUCTS, 3RD ED., J.F. Price and
B.S. Schweigert
HANDBOOK OF FOOD COLORANT PATENTS, F.J. Francis
ROLE OF CHEMISTRY IN THE QUALITY OF PROCESSED FOODS,
O.R. Fennema, W.H. Chang and C.Y. Lii
NEW DIRECTIONS FOR PRODUCT TESTING AND SENSORY ANALYSIS
OF FOODS, H.R. Moskowitz
PRODUCT TESTING AND SENSORY EVALUATION OF FOODS,
H.R. Moskowitz
ENVIRONMENTAL ASPECTS OF CANCER: ROLE OF MACRO AND MICRO
COMPONENTS OF FOODS, E.L. Wynder *et al.*
FOOD PRODUCT DEVELOPMENT IN IMPLEMENTING DIETARY
GUIDELINES, G.E. Livingston, R.J. Moshy, and C.M. Chang
SHELF-LIFE DATING OF FOODS, T.P. Labuza
RECENT ADVANCES IN OBESITY RESEARCH, VOL. V, E. Berry,
S.H. Blondheim, H.E. Eliahou and E. Shafir
RECENT ADVANCES IN OBESITY RESEARCH, VOL. IV, J. Hirsch *et al.*
RECENT ADVANCES IN OBESITY RESEARCH, VOL. III, P. Bjorntorp *et al.*
RECENT ADVANCES IN OBESITY RESEARCH, VOL. II, G.A. Bray
RECENT ADVANCES IN OBESITY RESEARCH, VOL. I, A.N. Howard
ANTINUTRIENTS AND NATURAL TOXICANTS IN FOOD, R.L. Ory
UTILIZATION OF PROTEIN RESOURCES, D.W. Stanley *et al.*
FOOD INDUSTRY ENERGY ALTERNATIVES, R.P. Ouellette *et al.*
VITAMIN B₆: METABOLISM AND ROLE IN GROWTH, G.P. Tryfiates
HUMAN NUTRITION, 3RD ED., F.R. Mottram
FOOD POISONING AND FOOD HYGIENE, 4TH ED., B.C. Hobbs *et al.*
POSTHARVEST BIOLOGY AND BIOTECHNOLOGY, H.O. Hultin and M. Milner

Newsletters

FOOD INDUSTRY REPORT, G.C. Melson
FOOD, NUTRITION AND HEALTH, P.A. Lachance and M.C. Fisher
FOOD PACKAGING AND LABELING, S. Sacharow

GUIDE FOR AUTHORS

Typewritten manuscripts in triplicate should be submitted to the editorial office. The typing should be double-spaced throughout with one-inch margins on all sides.

Page one should contain: the title, which should be concise and informative; the complete name(s) of the author(s); affiliation of the author(s); a running title of 40 characters or less; and the name and mail address to whom correspondence should be sent.

Page two should contain an abstract of not more than 150 words. This abstract should be intelligible by itself.

The main text should begin on page three and will ordinarily have the following arrangement:

Introduction: This should be brief and state the reason for the work in relation to the field. It should indicate what new contribution is made by the work described.

Materials and Methods: Enough information should be provided to allow other investigators to repeat the work. Avoid repeating the details of procedures which have already been published elsewhere.

Results: The results should be presented as concisely as possible. Do not use tables and figures for presentation of the same data.

Discussion: The discussion section should be used for the interpretation of results. The results should not be repeated.

In some cases it might be desirable to combine results and discussion sections.

References: References should be given in the text by the surname of the authors and the year. *Et al.* should be used in the text when there are more than two authors. All authors should be given in the Reference section. In the Reference section the references should be listed alphabetically. See below for style to be used.

DEWALD, B., DULANEY, J.T., and TOUSTER, O. 1974. Solubilization and polyacrylamide gel electrophoresis of membrane enzymes with detergents. In *Methods in Enzymology*, Vol. xxxii, (S. Fleischer and L. Packer, eds.) pp. 82-91, Academic Press, New York.

HASSON, E.P. and LATIES, G.G. 1976. Separation and characterization of potato lipid acylhydrolases. *Plant Physiol.* 57,142-147.

ZABORSKY, O. 1973. *Immobilized Enzymes*, pp. 28-46, CRC Press, Cleveland, Ohio.

Journal abbreviations should follow those used in *Chemical Abstracts*. Responsibility for the accuracy of citations rests entirely with the author(s). References to papers in press should indicate the name of the journal and should only be used for papers that have been accepted for publication. Submitted papers should be referred to by such terms as "unpublished observations" or "private communication." However, these last should be used only when absolutely necessary.

Tables should be numbered consecutively with Arabic numerals. The title of the table should appear as below:

Table 1. Activity of potato acyl-hydrolases on neutral lipids, galactolipids, and phospholipids

Description of experimental work or explanation of symbols should go below the table proper. Type tables neatly and correctly as tables are considered art and are not typeset. Single-space tables.

Figures should be listed in order in the text using Arabic numbers. Figure legends should be typed on a separate page. Figures and tables should be intelligible without reference to the text. Authors should indicate where the tables and figures should be placed in the text. Photographs must be supplied as glossy black and white prints. Line diagrams should be drawn with black waterproof ink on white paper or board. The lettering should be of such a size that it is easily legible after reduction. Each diagram and photograph should be clearly labeled on the reverse side with the name(s) of author(s), and title of paper. When not obvious, each photograph and diagram should be labeled on the back to show the top of the photograph or diagram.

Acknowledgments: Acknowledgments should be listed on a separate page.

Short notes will be published where the information is deemed sufficiently important to warrant rapid publication. The format for short papers may be similar to that for regular papers but more concisely written. Short notes may be of a less general nature and written principally for specialists in the particular area with which the manuscript is dealing. Manuscripts which do not meet the requirement of importance and necessity for rapid publication will, after notification of the author(s), be treated as regular papers. Regular papers may be very short.

Standard nomenclature as used in the engineering literature should be followed. Avoid laboratory jargon. If abbreviations or trade names are used, define the material or compound the first time that it is mentioned.

EDITORIAL OFFICES: DR. D.R. HELDMAN, COEDITOR, *Journal of Food Process Engineering*, Campbell Institute for Research and Technology, Campbell Place, Camden, New Jersey 08101 USA; or DR. R.P. SINGH, COEDITOR, *Journal of Food Process Engineering*, University of California, Davis, Department of Agricultural Engineering, Davis, CA 95616 USA.

CONTENTS

Conduction Heating of High Moisture Rough Rice
 II. Safe Temporary Storage
V.G. REYES, JR. and V.K. JINDAL 1

The Roast: Nonlinear Modeling and Simulation
M.A. TOWNSEND and S. GUPTA 17

A Finite Element Method to Model Steam Infusion Heat Transfer
 to a Free Falling Film
K.L. MCCARTHY and R.L. MERSON 43

A Generalized Viscosity Model for Extrusion of Protein Doughs
R.G. MORGAN, J.F. STEFFE and R.Y. OFOLI 55